

Persistence of a reef fish metapopulation via network connectivity: theory and data

Allison G. Dedrick^{a,*1}

Katrina A. Catalano^a

Michelle R. Stuart^a

J. Wilson White^b

Humberto Montes, Jr.^c

Malin Pinsky^a

a. Department of Ecology Evolution and Natural Resources, Rutgers University, 14 College Farm Road, New Brunswick, NJ 08901 USA;

b. Department of Fisheries and Wildlife, Coastal Oregon Marine Experiment Station, Oregon State University, Newport, OR 97365 USA;

c. Visayas State University, Pangasugan, Baybay City, 6521 Leyte, Philippines

* Corresponding author; e-mail: agdedrick@gmail.com

1. Current address: Stanford Woods Institute for the Environment, Stanford University, Stanford, CA 94305 USA.

Running title: (45 characters including spaces) Empirical metapopulation persistence

Keywords: metapopulation dynamics, self-persistence, network persistence, *Amphiprion clarkii*, connectivity (5/10)

Statement of authorship: MLP, JWW, and AGD conceived of and designed the study. MLP, MRS, KAC, and AGD conducted field work and collected data. HRM facilitated field work and provided local ecosystem context and knowledge. AGD analysed the data and wrote the first draft of the manuscript. All authors contributed substantially to revisions.

Data accessibility statement

Acknowledgements

We thank Visayas State University for providing logistical support and local ecosystem knowledge during our field sampling in Leyte, Philippines. We particularly thank Geralde Sucano, Jennifer Hoey, Patrick Flanagan, Joyce Ong, Apollo Lizano, Cecil Bantiles, Rodney Silvado, Beverlito Montalban, Teresita Idara, Rogello Nicanor, Liza Espinosa, Shem San Jose, Noel Alquino, Carlos Balasuna, Froilan Beas, Danilo Marine, Tony Nahacky, and Arturo Bastasa. For financial support, we thank Rutgers School of Environmental and Biological Sciences, NSF #OCE-1430218, and Alfred P. Sloan Research Fellowship, and an ORAU Ralph E. Powe Junior Faculty Enhancement award. This is publication number # of PISCO, the Partnership for Interdisciplinary Study of Coastal Oceans, funded primarily by the David and Lucile Packard Foundation.

Abstract

Determining whether a metapopulation can persist requires an understanding of both demographic parameters and connectivity among patches. This is well understood in theory but has proved challenging to test empirically. We assessed persistence for a network of patches along a coastline in a metapopulation of yellowtail anemonefish (*Amphiprion clarkii*) using seven years of annual sampling data. We found that this metapopulation produced enough surviving offspring to replace itself but that the spatial pattern of connectivity made it unlikely to persist in isolation despite stable abundances through time. To persist, the metapopulation would need higher fecundity or would need to retain essentially all of the recruits it produced. Increased habitat density alone would not ensure persistence. This first assessment of persistence in a marine metapopulation shows that stable abundance alone is not an indicator of persistence, emphasizing the necessity of untangling demographic and connectivity processes to understand metapopulation dynamics. (138/150 words)

Introduction

The dynamics and persistence of metapopulations depend both on connectivity among patches and on demographic rates within each patch (Hastings and Botsford, 2006; Hanski, 1998). For marine species, connectivity among habitat patches primarily occurs during planktonic larval stages when individuals are hard to track and are able to travel long distances with ocean currents. Because larval connectivity has been perceived to be the greatest uncertainty in these systems, research

has centered on quantifying that component (reviewed by White et al., 2019). More recently, it has become apparent that variation in demographic rates among patches is an equally uncertain aspect of marine metapopulation dynamics (Hameed et al., 2016; White and Samhouri, 2011). Given both of those uncertainties, and driven by both fundamental ecological questions and applied needs (Botsford et al., 2001; White et al., 2010), a large body of theory has developed to describe how connectivity and local demography interact to determine whether marine metapopulations persist (Burgess et al., 2014; Botsford et al., 2019). Testing this theory, however, has proven substantially more difficult.

For any population to persist, individuals must on average replace themselves during their lifetime. Assessing replacement must account for demographic processes across the life cycle, including how likely individuals are to survive to the next age or stage, their expected fecundity at each stage, and the survival to recruitment of any offspring produced. In a spatially structured population, how the offspring are distributed across space is also important (Hastings and Botsford, 2006).

A metapopulation can persist via two mechanisms: 1) at least one patch achieves replacement in isolation, or 2) multiple patches receive enough recruitment to achieve replacement through multi-generational loops of connectivity with other patches in the metapopulation (Hastings and Botsford, 2006; Burgess et al., 2014). In the first case (termed self-persistence), enough of the offspring produced at one patch are retained there for it to persist. In the second case (network persistence), closed loops of connectivity among patches - in which offspring from one patch recruit to another patch but eventually send offspring back to the first in a future generation - provide

the patches with enough recruitment to persist within the network. Theory predicts that habitat patches that are large relative to the mean dispersal distance are likely to be self-persistent (White et al., 2010).

New ways of identifying individuals and determining their origins now allow better measurements of connectivity in marine populations (Almany et al., 2017; D'Aloia et al., 2013). Additionally, a better appreciation of the relevant population dynamic theory has led to measurement of the appropriate demographic factors necessary to assess persistence in field metapopulations (Carson et al., 2011; Hameed et al., 2016; Johnson et al., 2018; Salles et al., 2015). To date, research has suggested that populations on isolated islands can be self-persistent, which might be expected given that they lack nearby populations from which to receive larvae and would go locally extinct if they did not achieve replacement Salles et al. (2015). In contrast, small habitat patches spread across a larger reef metapopulation appear to rely on input from surrounding and intervening patches for persistence (Johnson et al., 2018). Persistence, however, has yet to be quantified in the field for an entire continuous marine metapopulation, such as all of the patches along a coastline.

Here, we further our understanding of metapopulation dynamics in a network of patches along a coastline through a study of yellowtail anemonefish (*Amphiprion clarkii*) in the Philippines. We assessed persistence for all patches of habitat within a metapopulation spread across 30 km of coastline. Based on seven years of data, we found that, despite containing multiple patches with large abundances that were stable over time, the metapopulation was not likely to be persistent and requires immigration from outside patches to persist.

Methods

Persistence theory and metrics

We considered four primary metrics to assess whether and how the anemonefish metapopulation was persistent: 1) lifetime recruit production (LRP) to assess whether the metapopulation had enough offspring that survived anywhere to achieve replacement, 3) self-persistence (SP) to assess whether any individual patch could persist in isolation without input from other patches, 3) network persistence (λ_c) to assess whether the metapopulation was persistent as a connected unit, and 4) local replacement (LR) to assess whether a sufficient number of recruits were retained anywhere within the metapopulation to achieve replacement, without explicitly estimating dispersal. We explain each metric below in detail. To represent the uncertainty in our estimates, we calculated each metric 1000 times, sampling each input parameter from a distribution representing the uncertainty in the empirical estimate (details in A.9). In our results, we show best estimates of each metric with the range of uncertainty values along with uncertainty bounds, defined as the middle 95% of the distribution of values calculated in this Monte Carlo procedure.

Lifetime recruit production

LRP_i is the expected number of recruits a recruit on patch i will produce in its lifetime,

$$\text{LRP}_i = \text{LEP}_i \times S_e, \quad (1)$$

where LEP_i (lifetime egg production) is the patch-specific number of eggs a recruit produces in its lifetime and S_e (egg-recruit survival) is the fraction of eggs that survive to become recruits (Fig. D.1).

If $\text{LRP} \geq 1$, individuals produced enough surviving offspring, before considering dispersal, to potentially achieve replacement. If $\text{LRP} < 1$, the population could not persist without input from outside patches. We considered all recruits produced by adults in our metapopulation to estimate LRP_i , regardless of where they settled.

Self-persistence

SP_i is the number of offspring a recruit produces that survive to recruitment and settle in the natal patch,

$$\text{SP}_i = \text{LRP}_i \times p_{i,i}, \quad (2)$$

where $p_{i,i}$ is the probability of larval retention on patch i .

A patch i is self-persistent if $\text{SP}_i \geq 1$. If at least one patch is self-persistent, the metapopulation as a whole persists as well (Hastings and Botsford, 2006; Burgess et al., 2014).

Network persistence

Network persistence is the largest real eigenvalue λ_C of the realized connectivity matrix C ,

$$C_{i,j} = \text{LRP}_i \times p_{i,j}, \quad (3)$$

which we created by multiplying lifetime recruit production (LRP_i) by dispersal probabilities among pairs of patches ($p_{i,j}$) (Burgess et al., 2014). The diagonal entries of C are the self-persistence values for each individual patch (SP_i).

Network persistence explicitly considers dispersal of individuals among patches in addition to the reproduction and survival at each patch and requires $\lambda_C \geq 1$ for the network to persist without outside input (Hastings and Botsford, 2006; White et al., 2010; Burgess et al., 2014).

Local replacement

Local replacement (LR) is the number of recruits a recruit produces that return to settle within the focal metapopulation. LR is related to LRP, but LRP, in contrast also includes recruits that settle outside of the focal metapopulation. LR is define as

$$\text{LR} = \text{LEP}_* \times R_e, \quad (4)$$

where LEP_* is lifetime egg production averaged across sites and R_e is the proportion of eggs that survived and returned to recruit at the patches in our focal

metapopulation (the 30 km section of coastline). R_e is a modification of egg-recruit survival (S_e) that implicitly includes dispersal.

If $LR \geq 1$, enough offspring were locally retained to achieve replacement if they were evenly spread among patches, but the actual dispersal patterns among the metapopulation patches may still prevent replacement if the pattern of multigenerational replacement does not satisfy the Hastings and Botsford (2006) criterion. LR and λ_c both assess the ability of our patches to persist as an isolated group but LR treats the network as one large homogenous patch while λ_c explicitly accounts for the structure and connectivity among patches.

Study species

We focused on a tropical metapopulation of yellowtail anemonefish (*Amphiprion clarkii*, Fig. 2c). Like many anemonefish species, yellowtail anemonefish have a mutualistic relationship with anemones that house small colonies of fish (Buston, 2003b; Fautin et al., 1992). Yellowtail anemonefish are protandrous hermaphrodites and maintain a size-structured hierarchy; within an anemone, the largest fish is the breeding female, the next largest is the breeding male, and any smaller fish are non-breeding juveniles. The fish move up in rank to become breeders only after the larger fish have died. In the tropical patch reef habitat of the Philippines, yellowtail anemonefish primarily spawn from November to May and lay clutches of benthic eggs that the parents protect and tend (Ochi, 1989; Holtswarth et al., 2017). Larvae hatch after about six days and spend 7-10 days in the water column before returning to reef habitat to settle in an anemone (Fautin et al., 1992).

Anemonefish are well-suited to metapopulation studies because dispersal only occurs during the larval phase and adults have limited movement on discrete habitat patches (anemones) (e.g., Buston and DAloia, 2013; Salles et al., 2015; Almany et al., 2017). Yellowtail anemonefish tend to behave more like other reef fishes, with wider-ranging territories and stronger swimming abilities (Hattori and Yanagisawa, 1991; Ochi, 1989), than the smaller *A. percula* commonly used in metapopulation studies (e.g. Buston et al., 2011; Salles et al., 2015).

Field data collection

We focused on a set of nineteen reef patches spanning 30 km along the western coast of Leyte island facing the Camotes Sea in the Philippines (Fig. 2a). The habitat patches covered approximately 20% of the sampling region and consisted of rocky patches of coral reef separated by sand flats (Fig. 2a,b). To the north, the patches were isolated from nearby habitat with no substantial reef habitat for at least 20 km, a distance greater than the mean dispersal distance for this species (Pinsky et al., 2010). As such, we considered this to be a relatively isolated metapopulation. Located near a populated coastline, the region experiences anthropogenic effects including fishing, pollution, and runoff from agriculture and a nearby riverbed gravel mine as well as reef-destroying storms like Haiyan and other typhoons in 2013.

From 2012-2018, we sampled fish and habitat at most patches each year (Table A4). Divers using SCUBA and tethered to GPS readers swam the extent of each patch and visited anemones inhabited by yellowtail anemonefish. At each anemone, the divers caught fish 3.5 cm and larger, took a tissue sample, measured fork length,

and noted tail color as an indicator of life stage. Starting in 2015, fish 6.0 cm and larger were also tagged with a passive integrated transponder (PIT) tag unless already tagged. Divers also looked for eggs around each anemone and measured and photographed any clutches found. In total, we took fin clips from and genotyped 2407 fish and PIT-tagged 1930 fish across all years and patches combined, marking 3053 individual fish.

Estimating demographic and dispersal parameters from empirical data

Parentage analysis and dispersal kernel

Over seven years of sampling, we genotyped 1719 potential parents and 785 juveniles at 1340 single nucleotide polymorphisms (SNPs) and found 62 parent-offspring matches (Catalano et al., in prep). We used a distance-based dispersal kernel fit from the parent-offspring matches (Catalano et al., in prep; Bode et al., 2018), where the relative dispersal $p(d)$ is a function of distance d in kilometers and parameters θ and $z = e^{K_d}$ that control the shape and scale of the kernel (Table A1, uncertainty details in SI A.9.0.1). The dispersal kernel estimates the relative dispersal by distance for fish that have survived and recruited so does not separately estimate pre-settlement mortality. To find the probability of fish dispersing among our patches, we numerically integrated the dispersal kernel using the distance from the middle of the origin patch (i) to the closest (d_1) and farthest (d_2) edges of the destination patch (j), with distances calculated using the `geosphere` package in R (Hijmans, 2017):

$$p_{i,j} = \frac{z\theta}{2\gamma(\frac{1}{\theta})} \int_{d_1}^{d_2} ze^{-(zd)^\theta} dd. \quad (5)$$

Growth and survival: mark-recapture analyses

Fish marked through geneotyping and PIT tags allowed us to estimate growth and survival through mark-recapture. In total, we had 3053 marked fish with size and stage data for each capture time.

For growth, we used a von Bertalanffy growth curve

$$\begin{aligned} L_{t+1} &= L_t + (L_\infty - L_t)[1 - e^{(-k)}] \\ &= e^{(-k)}L_t + L_\infty[1 - e^{(-k)}], \end{aligned} \quad (6)$$

where L_∞ is the asymptotic maximum size across the metapopulation and k is the growth rate. We estimated the parameters from the slope m and y-intercept b of the relationship between the length at first capture L_t and the length at a later capture date L_{t+1} for fish recaptured after a year (within 345 to 385 days). The von Bertalanffy parameters are $k = -\ln m$ and $L_\infty = b(1 - m)$ (Hart and Chute, 2009) (Fig. 3b, Table A1, uncertainty details in SI A.9.0.2).

We used the full set of marked fish to estimate annual survival ϕ and probability of recapture p_r using the mark-recapture program MARK implemented in R through the package `RMark` (Laake, 2013). We fit several models with year, size, and patch effects on the probability of survival on a log-odds scale (see details in SI A.4 and

full list of models in Table A3). The model chosen by AIC_c indicated that survival differed among patches and increased with fish size (Tables A1, A2, Figs. 3c, D.5, uncertainty details in SI A.9.0.3).

Fecundity

From a regression of eggs per clutch on female size and egg age (determined by the presence of eyed eggs), we determined that fecundity increased with size (eqn. A.1, see details in SI A.5). We only considered reproductive effort once the fish is female and used the average size of first female observation for recaptured fish as the transition size L_f (Fig. 3d, uncertainty details in SI A.9.0.4).

Lifetime egg production (LEP)

We used an integral projection model (IPM) (Ellner et al., 2016) with size as the continuous structuring trait L to estimate lifetime egg production on each patch i (LEP_i). We initialized the IPM with one recruit-sized individual (recruit defined in SI A.1) at the initial annual time step ($t = 0$), then projected forward for 100 years. We used the size-dependent survival (eqn. B.1) and growth (eqn. 6) functions as the probability density functions in the kernel to project the individual into the next time step. The size distribution (v_z) at each time step represents the probability that the individual has survived and grown into each of the possible size categories, ranging from a minimum of $L_s = 0$ cm to a maximum of $U_s = 15$ cm divided into 100 equal size bins.

We then multiplied the size-distribution v_L at each time by the size-dependent

fecundity f (eqn. A.1) to get the total number of eggs produced at each time step. Integrating across time and size gave the total number of eggs one recruit produced in its lifetime (details in A.6, uncertainty details in SI A.9.0.5):

We calculated LEP by site (LEP_i) and averaged across sites (LEP_*) starting for a fish of recruit size. We also calculated LEP averaged across sites for a fish starting a parent size (6.0cm) (LEP_p), used below to estimate egg-recruit survival.

$$\text{LEP} = \int_{t=0}^{100} \int_{L=L_s}^{L=U_s} v_{L,t} f_L dL dt. \quad (7)$$

Accounting for density-dependence

We would ideally assess persistence metrics when the population is at low abundance and not limited by density dependence because persistence is defined as having positive population growth at low density; at high density the population growth rate will slow to zero. Density dependence is particularly clear in anemonefish, which have strong social hierarchies. Juveniles on an anemone will prevent others from settling there as well (seen in *A. percula*, Buston, 2003a). Each anemone, therefore, can house only one recently settled anemonefish. This density-dependent mortality artificially reduces the apparent survival of new recruits (recruit defined in SI A.1), likely biasing persistence metrics. We accounted for this effect by scaling up our estimate of recruits (the numerator of eqn. 8, described next) by the proportional increase (DD) in unoccupied anemones if all of the anemones occupied by yellowtail anemonefish were unoccupied, where p_A is the proportion of anemones oc-

cupied by yellowtail anemonefish and p_U is the proportion of unoccupied anemones: $DD = \frac{(p_U+p_A)}{p_U} = 1.81$. We present results with this density-dependence modification in the main text and without in the appendix (with subscript DD, Figs. D.9, D.10).

Survival from egg to recruit (S_e)

We estimated survival from egg to recruit (S_e) using parentage matches to find the number of surviving recruits produced by genotyped parents (similar to Johnson et al., 2018). However, the number of offspring we assigned back to parents ($R_m = 71$) is a severe underestimate of the offspring produced by genotyped parents because we could not sample exhaustively. To account for offspring missed by our sampling, we divided R_m by four factors (described below and with details in SI A.8 and in diagram Fig. D.2), in addition to multiplying by DD as described above, then divided by the number of eggs produced by genotyped parents:

$$S_e = \frac{\frac{DDR_m}{P_h P_c P_d P_s}}{N_g \text{LEP}_p}, \quad (8)$$

where N_g (=1729) was the number of genotyped parents and LEP_p was the expected lifetime egg production for a fish that has already survived to parent size p (=6.0cm). LEP_p therefore does not include survival from recruit to parent sizes. P_h (=0.41) was the cumulative proportion of habitat in our patches that we sampled over time (details in SI A.8.0.1), P_c (=0.56) was the probability of capturing a fish if we sampled its anemone (details in SI A.8.0.2), P_d (=0.57) was the proportion of the total dispersal kernel area from each of our patches covered by our sampling region

(details in SI A.8.0.3), and P_s ($=0.20$) was the proportion of suitable habitat in our sampling region (details in SI A.8.0.4).

To estimate the survival and retention of recruits back to our patches (needed for local replacement, LR eqn. 4), we scaled only by P_h and P_c :

$$R_e = \frac{\frac{DDR_m}{P_h P_c}}{N_g \text{LEP}_p}. \quad (9)$$

Estimated abundance over time

We examined trends in abundance of breeding females at each patch over time ($F_{i,t}$) to compare to our replacement-based persistence estimates. As with offspring, we scaled up the number of females caught ($F_{c_{i,t}}$) at each patch i in each sampling year t by the proportion of habitat sampled in that patch and year ($P_{h_{i,t}}$) and by the probability of capturing a fish P_c :

$$F_{i,t} = \frac{F_{c_{i,t}}}{P_{h_{i,t}} P_c} \quad (10)$$

We fit a mixed effects model to estimate the number of fish in each year as a Poisson-distributed variable λ_a with effect m_t of year t and with patch as a random effect m_i using the package `lme4` in R (Bates et al., 2015):

$$\begin{aligned} F_{i,0} &\sim \text{Poisson}(\lambda_a) \\ F_{i,t} &= (\lambda_a + m_i)m_t. \end{aligned} \quad (11)$$

We estimated λ_a for an average patch as well as the individual patches.

Exploring alternative geographies and larval navigation

Finally, we tested the sensitivity of metapopulation persistence to patch width and to the proportion of the region that is habitat to understand whether the results would likely be similar in other geographies. We varied the proportion of habitat and the overall width of the region using 19 equally sized and spaced patches with adult survival from the patch with median survival (Elementary School). We created connectivity matrices using the new distances between patches and otherwise used the original parameter values and uncertainty sets.

We also tested sensitivity to the ability of larvae to navigate to habitat by adding up to a 1km buffer to the edges of the destination patches when integrating the dispersal kernel and adjusting the scaling parameter P_s (eqn. 8) to account for fewer larvae being lost between patches (details in SI A.7.0.1).

Results

Demographic rates

From field data, mark-recapture, and parentage analyses, we estimated growth, annual survival, and egg-recruit survival. We found an average asymptotic maximum size L_∞ of 10.7 cm, with a growth rate $k = 0.86$ (Fig. 3b, details in SI B.2). Annual survival varied by site and was higher for larger fish (Figs. 3c and D.5, Table A2, details in SI B.3). Average lifetime egg production across sites (LEP_*) was 827

[227, 2919] (Fig. 4a, details in SI B.4). Egg-recruit survival was 0.002 [0.0005, 0.01] (details in SI B.5). Catalano et al. (in prep) estimated the dispersal kernel we used, finding a mean dispersal distance of 8.15 km (Fig. 3a).

Persistence metrics

Using our estimates of growth, survival, fecundity, dispersal, and density dependence, we estimated average lifetime recruit production across patches to be 1.74 [0.94, 5.68] (Fig. 4b). Estimates of LRP_i at individual patches ranged from 0 to 3.7 (Table A5, Fig. D.8). Averaged across patches, 95% of LRP estimates were ≥ 1 , which means that individuals produced enough offspring to replace themselves. However, LRP does not tell us whether those offspring settled in locations that contributed to persistence.

Considering retention of larvae at individual patches, we did not find any patches with $SP_i \geq 1$ (Fig. 5a), suggesting that no patch could persist in isolation. The Haina patch came closest to but was still far from self-persistence ($SP_i = 0.044$ [0.005, 0.23]).

For network persistence, our estimate of λ_c was 0.18 [0.09, 0.63]. None of the uncertainty distribution of λ_c was ≥ 1 (Fig. 5c), suggesting network persistence for this metapopulation was therefore extremely unlikely if not impossible. Our estimate of local replacement (LR) was 0.20 [0.11, 0.65], also suggesting lack of independent persistence of our group of patches and very similar to our λ_c estimate. While both LR and λ_c provide information on the ability of our patches to persist as an isolated group, they differ in their assumption of the structure of the population. LR approx-

imates the network of patches as a single well-mixed unit, while λ_c incorporates the spatial structure of the patches and multi-generation dynamics.

Abundance

Our estimated abundance of females over time had a slight positive trend for the average patch ($m_t = 1.08$, Fig. 4a), suggesting a slight increase in population size through time. Most individual patches also showed a slight positive trend in female abundance through time, though one large patch (Sitio Baybayon) showed declines (Figs. 4a, D.7s). Therefore, though the metapopulation did not exhibit network persistence, it also did not show signs of decline over the time scale of our study.

Alternative geographies

We then examined what conditions would be needed for this metapopulation to reach persistence. With the existing patch configuration and dispersal kernel, the system would need $LRP \geq 8.9$ (a five-fold increase) to reach network persistence. In turn, this would require a five-fold increase of egg-recruit survival (S_e) or LEP_* or an equivalent combination of increases across both. Including all arriving recruits as offspring, not just those originating within the metapopulation, LRP would be 11.1, sufficient for persistence. Similarly, our estimate of LR using all recruits arriving to the patches gave an estimate > 1 (2.21), also suggesting there was recruit-recruit replacement for the metapopulations when immigrants were included.

Another route to persistence would be with a different dispersal matrix. If dispersal was such that the metapopulation retained all offspring produced, the study

region would be persistent because $\text{LRP} > 1$. With the observed dispersal pattern, however, retaining all recruits is difficult to achieve. The coastline had a low fraction of habitat (20%) and would need to be increased to about 86% habitat before enough offspring are retained for persistence and the estimate of $\lambda_c > 1$ (with a majority of estimates ≥ 1 , Fig. 6a). However, widening the region while maintaining the same habitat density (20%) did not achieve persistence (Fig. 6b) unless habitat density was also increased (Fig. 6c). As the region widens, the habitat density necessary for persistence decreases, down to 74% habitat at a region of 50 km. In contrast, allowing for larval navigation had little impact on persistence estimates (Fig. 6d), as the larger effective area of each patch was essentially offset by removing that area from the scaling that accounted for larval losses to non-habitat (P_s in eqn. 8).

Discussion

In this first assessment of demographic persistence of a coastal marine metapopulation, we did not find strong evidence for either self-persistence of an individual patch or network persistence of the entire 30 km area as an isolated region. This inability to persist as an isolated region does not mean that the metapopulation was declining, however. Both population trends and replacement of recruits with immigrants showed that population levels were stable or increasing slightly. Taken together, these metrics suggest that the region required input of immigrants to persist. Despite encompassing a distance substantially larger than mean dispersal, the coastline only persisted as part of a larger metapopulation.

Theory for predicting persistence within patchy habitats has suggested that we

expect self persistence for patches with a length at least twice the mean dispersal distance (Lockwood et al., 2002) and network persistence from groups of patches where the proportion of habitat is about 10-40% (depending on the particular species, population, and the steepness of the stock-recruit curve, Botsford et al., 2019). Individual patches in the focal metapopulation were too small for self-persistence, but the 30 km region we sampled was about triple the mean dispersal distance of yellowtail anemonefish estimated from previous genetic work (around 9 km, Pinsky et al., 2010) and from our parentage analyses (8.2 km, Catalano et al., in prep). Rather than a continuous patch, however, the region was only about 20% habitat. This low value may result at least in part from habitat declines over recent decades, based on interviews with fishers in the early 2000s (Jennifer Selgraeth, pers. comm.). Increasing the proportion of coastline with habitat in sensitivity tests, however, suggested that 40% habitat coverage would not be sufficient to achieve persistence and this metapopulation would require at least 86% habitat to persist. Similar to fish on small patches in the Caribbean (Johnson et al., 2018), this anemonefish metapopulation depends on the production and connectivity of outside patches. One possible path to persistence would be through nearby patches that had higher egg production or survival. In such a case, even a small increase in area could create a persistent network. Deeper reefs, for example, often have better reef health than shallower reefs (Cinner et al., 2016) - LRP_i is highest at our deepest patch, Tomakin Dako. In our system, offshore reefs at Cuatro Islas or the Camotes Islands, for example, with higher coral cover and less silt, could have higher anemonefish survival and contribute disproportionately to regional metapopulation persistence.

Our finding of a lack of isolated persistence of differs markedly from persistence findings of other reef fish metapopulations. On reefs surrounding Kimbe Island, Salles et al. (2015) report self-persistence of individual anemonefish subpopulations in lagoons that were of similarly size (approximately 100-500 m long) to our individual patches, as well as network persistence of the only 800 m wide metapopulation around the island. This persistence finding is at a dramatically smaller scale than for our focal population in the Philippines. Additionally, Johnson et al. (2018) estimated that four reefs of a combined area of only 2.6 km^2 (4 65 ha patches) would be sufficient for network persistence of a damselfish metapopulation across multiple islands in the Bahamas. This area is equivalent to a coastline section shorter than our sampling region (approximately 30 km long and 0.1 km wide). To persist, these two offshore metapopulations either had much higher retention of recruits or higher LRP than did our coastline patches. Though lack of sufficient connectivity and retention is thought to inhibit network persistence in some systems (e.g., insufficient retention of offspring within reserves for eastern oysters (*Crassostrea virginica*) in North Carolina; Puckett and Eggleston, 2016), production of surviving recruits seems the likelier explanation in this case. Recruit production was lower in the Philippines than in the Kimbe Island populations, where estimates of lifetime reproductive success that included dispersal to the natal reef (Salles et al., 2020) were higher than our estimates of LRP without dispersal losses (LRP of 1.74). Lower LRP at our sites could be due to lower egg production, slower growth, or lower adult survival, all likely affected by habitat quality (e.g. Salles et al., 2020; Hayashi et al., 2019). Our study system was near a populated coastline and experienced anthropogenic effects,

including pollution and silt, that can reduce demographic rates. Adult survival, for example, was lower at the two patches just downstream of the gravel mine (N. and S. Magbangon in Fig. B.3). Even at our higher-survival sites, survival was lower than estimates from the populations at Kimbe Island (85% annual survival, Salles et al., 2015). Metapopulation studies in other reef fish (e.g. Figueira, 2009) and marine species more broadly (Carson et al., 2011) are highly sensitive to adult survival and other demographic parameters. Temporal variability in demographic or dispersal parameters on a time scale longer than our sampling alternatively could have enabled persistence of our patches in isolation (similar to the storage effect, Warner and Chesson, 1985) rather than as part of a larger metapopulation. Successful recruitment events on the decadal scale, for example, sustain rockfish populations on the west coast of the United States through the intervening weak recruitment years (e.g. Tolimieri and Levin, 2005). Our study could have missed a particularly strong recruitment event driven by variable ocean connectivity (simulations suggest that 20 years are necessary to capture the full extent of ocean variability in the Coral Triangle region surrounding our patches; Thompson et al., 2018). Strong recruitment would need to occur at least once a generation to maintain patch populations without switching to colonization and extinction dynamics, however, which we do not see. Our study likely spans the generation time of a yellowtail anemonefish (roughly 5 years) so variable strong recruitment, while possible, is unlikely to sustain our populations.

Understanding our region in the context of broader metapopulation theory requires reconciling replacement-based persistence analysis with classic colonization-

extinction and source-sink dynamics. At the patch level, many marine metapopulations do not exhibit the colonization-extinction dynamics (or do only on a decades to centuries timescale, Smedbol et al., 2002) more common in terrestrial metapopulations (e.g. in butterflies and pikas; Hanski, 1998; Moilanen et al., 1998) and instead consist of continuously occupied patches connected by dispersal (Kritzer and Sale, 2006) that are not necessarily easily classified as sources or sinks. Despite being unable to persist in isolation, our region is not technically a sink (Pulliam, 1988) because $LRP > 1$. For these metapopulations, lack of self-persistence can have two causes: reproduction does not balance mortality losses within a patch (as in a sink) or sufficient recruits are produced but not retained (as we see in our region). Dispersal that leads to demographic exchange rather than colonization is not commonly considered in classic metapopulation dynamics, though there have been some attempts to include all successful offspring from a patch and not just those retained locally when classifying sources and sinks (Figueira and Crowder, 2006). Many metapopulations likely lie on a continuum between extinction-colonization dynamics and exchange among populated patches (Kritzer and Sale, 2006), and bridging these metapopulation views could lead to a more complete understanding of persistence in patchy and variable environments.

Our sampling on patchy coral reefs was designed for mark-recapture analysis rather than a comprehensive habitat or abundance census, so though we accounted for uneven sampling, we could have missed population declines if the underlying habitat was shifting. We used tagged anemones to account for unvisited patch habitat, but tags with missing anemones are harder to find. If anemones disappeared

over time at our patches, we could have overestimated the number of fish and missed population declines indicating lack of persistence even with outside input. These scaling challenges are not unique to our study: few ecological studies are full censuses through time, and marine metapopulations tend to be patchy and heterogeneous (e.g. coral reefs, the intertidal zone, and kelp forests; Saenz-Agudelo et al., 2011; Johnson, 2001; Castorani et al., 2015), where individuals are not well-mixed across space or time. In these cases, carefully considering how sampling interacts with distribution, properly accounting for such uncertainties, and characterizing uncertainty in parameter estimates, is an important part of persistence estimation.

Density-dependence also presents a sampling challenge. Persistence criteria (Hastings and Botsford, 2006; Burgess et al., 2014) ask whether a population at low abundance can grow and recover rather than going extinct. Density-dependence is often ignored at low abundances (Botsford et al., 2019) so is not explicitly considered in persistence metrics. In real populations, however, it can be challenging to estimate density-independent demographic rates, as density-dependence is occurring in the population as it is sampled in processes such as dispersal (e.g. in butterflies, Nowicki and Vrabec, 2011) and fecundity (e.g. in warblers, Rodenhouse et al., 2003). In yellowtail anemonefish, density-dependence is likely most important immediately post-settlement, as it is for many species (e.g. corals, trees, and butterflies; Vermeij and Sandin, 2008; Harms et al., 2000; Nowicki et al., 2009), but could continue to be important throughout the life history due to social hierarchies in anemonefish colonies (e.g. Buston and Elith, 2011). To avoid competition within the colony, fish in the pre-reproductive queue may have lower growth and survival than fish alone

on an anemone (seen in *A. percula*, Buston, 2003b,a), suggesting higher growth and survival, and therefore LRP, in the absence of density-dependence.

Understanding persistence is critical for the management of spatial populations, such as siting marine protected areas (e.g. Kaplan et al., 2009), assessing habitat fragmentation risks (e.g. Smith and Hellmann, 2002; Fahrig, 2001) and conserving species in the face of climate change (e.g. Coleman et al., 2017; Fuller et al., 2015). Though models and theory provide us with expectations, we are only recently beginning to be able to tackle these questions of persistence empirically in model systems such as anemonefish and other sedentary tropical reef fish (e.g. Salles et al., 2015; Johnson et al., 2018). With parentage analyses now being extended to temperate marine species (e.g. Baetscher et al., 2019) and a better understanding of how bio-physical models compare to larval dispersal patterns (Bode et al., 2019), we are beginning to move beyond model species and investigate persistence in harvested and spatially-managed systems (e.g. Garavelli et al., 2018). Our study shows the importance of long term sampling and careful consideration of the different demographic processes that affect our metric calculations, such as density-dependence and sampling biases, to distinguish persistence ability from population trajectories and understand marine population dynamics in empirical systems.

Figures

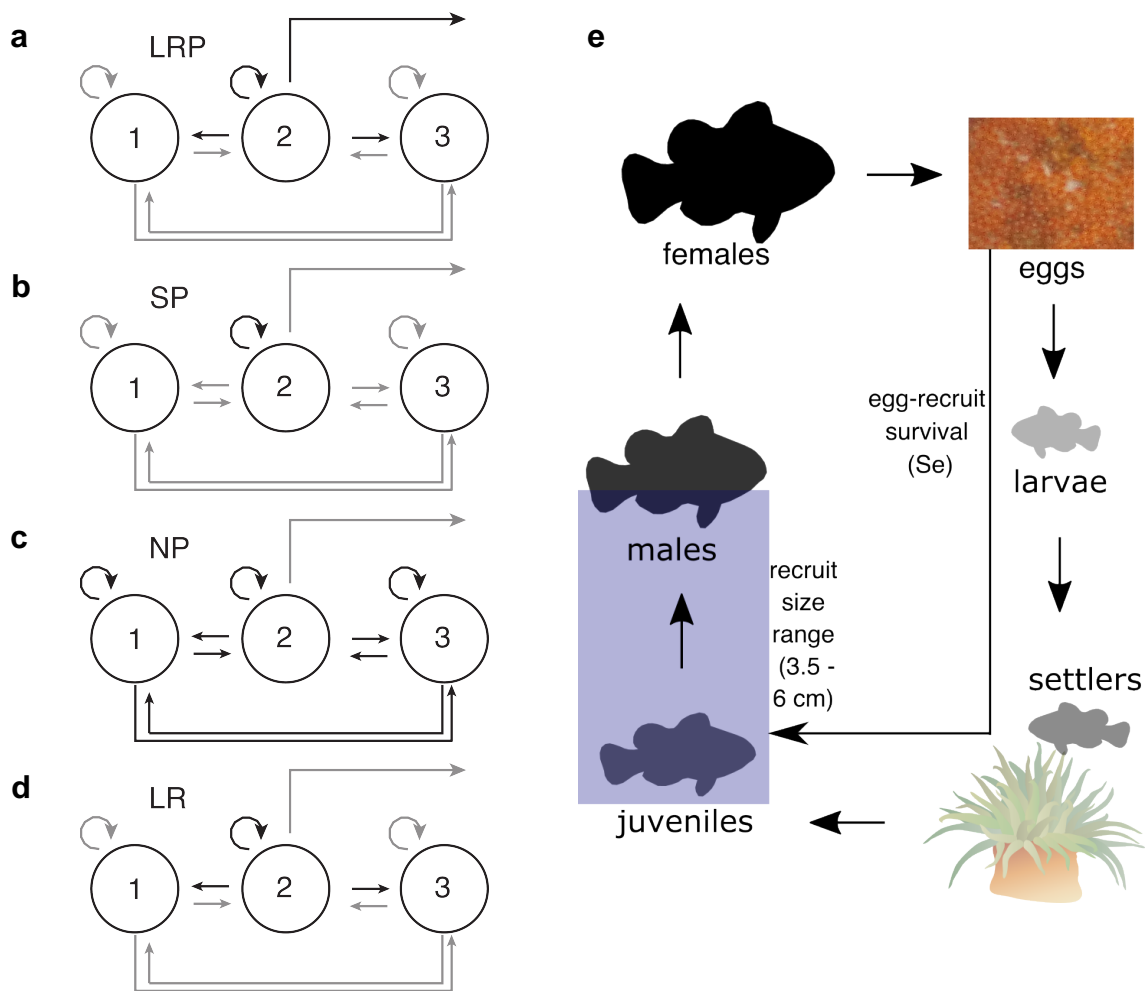


Figure 1: Schematics of the persistence metrics (a-d): a) lifetime recruit production (LRP, eqn. 1), b) self-persistence (SP, eqn. 2), c) network persistence (NP, first eigenvalue of eqn. 3), and d) local replacement (LR, eqn. 4). e) The life cycle of yellowtail clownfish, including the range of sizes considered recruits (recruit definition in SI A.1).

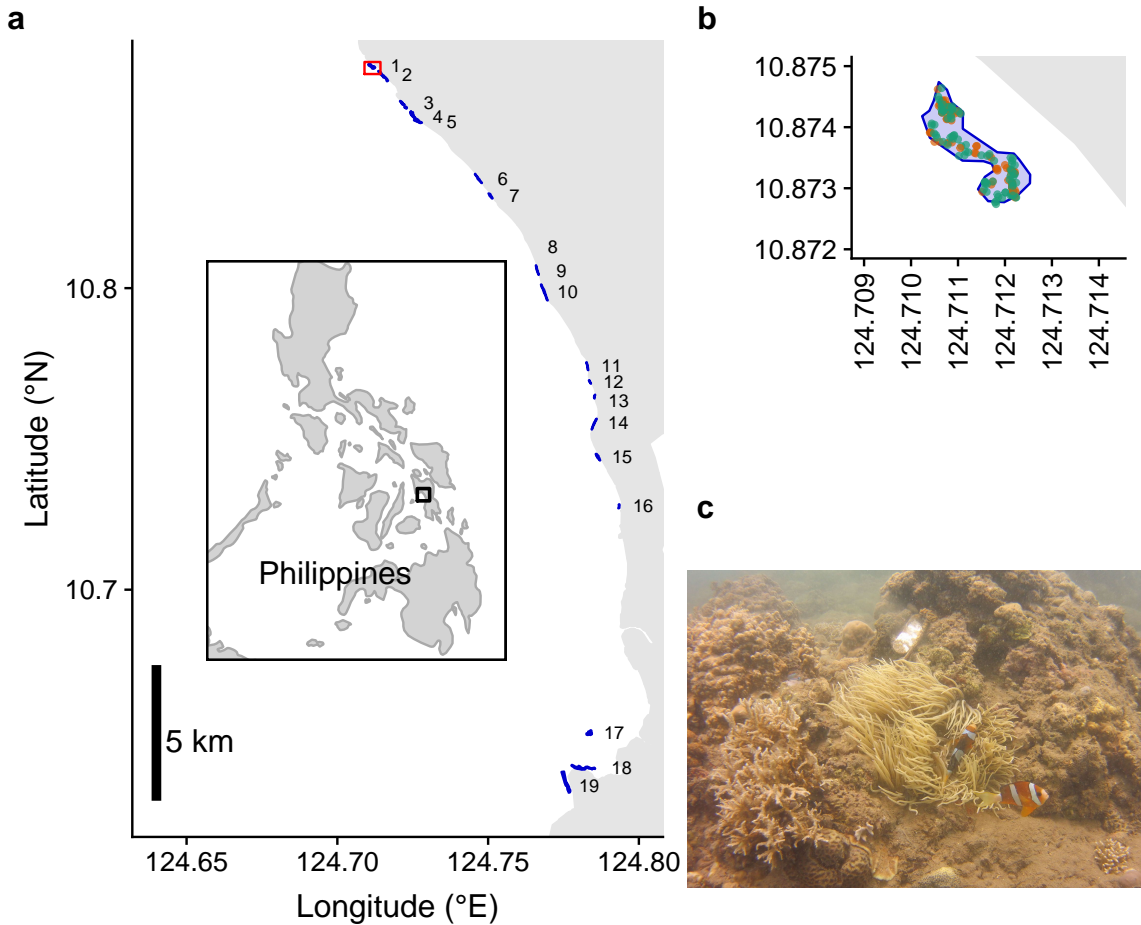


Figure 2: a) Map of the patches along the coast of Leyte in the Philippines. From north to south, the patches are: 1) Palanas, 2) Wangag, 3), North Magbangon, 4) South Magbangon, 5) Cabatoan, 6) Caridad Cemetery, 7) Caridad Proper, 8) Hicgop South, 9) Sitio Tugas, 10) Elementary School, 11) Sitio Lonas, 12) San Agustín, 13) Poroc San Flower, 14) Poroc Rose, 15) Visca, 16) Gabas, 17) Tomakin Dako, 18) Haina, and 19) Sitio Baybayon. b) Zoomed-in map of the northern-most patch, Palanas, to show anemone arrangement with anemones colored as occupied by *A. clarkii* (green) or unoccupied by anemonefish (orange). c) An example anemone occupied by *A. clarkii* in a typical habitat at the patches. The metal anemone tag is visible just above the anemone on the rock.

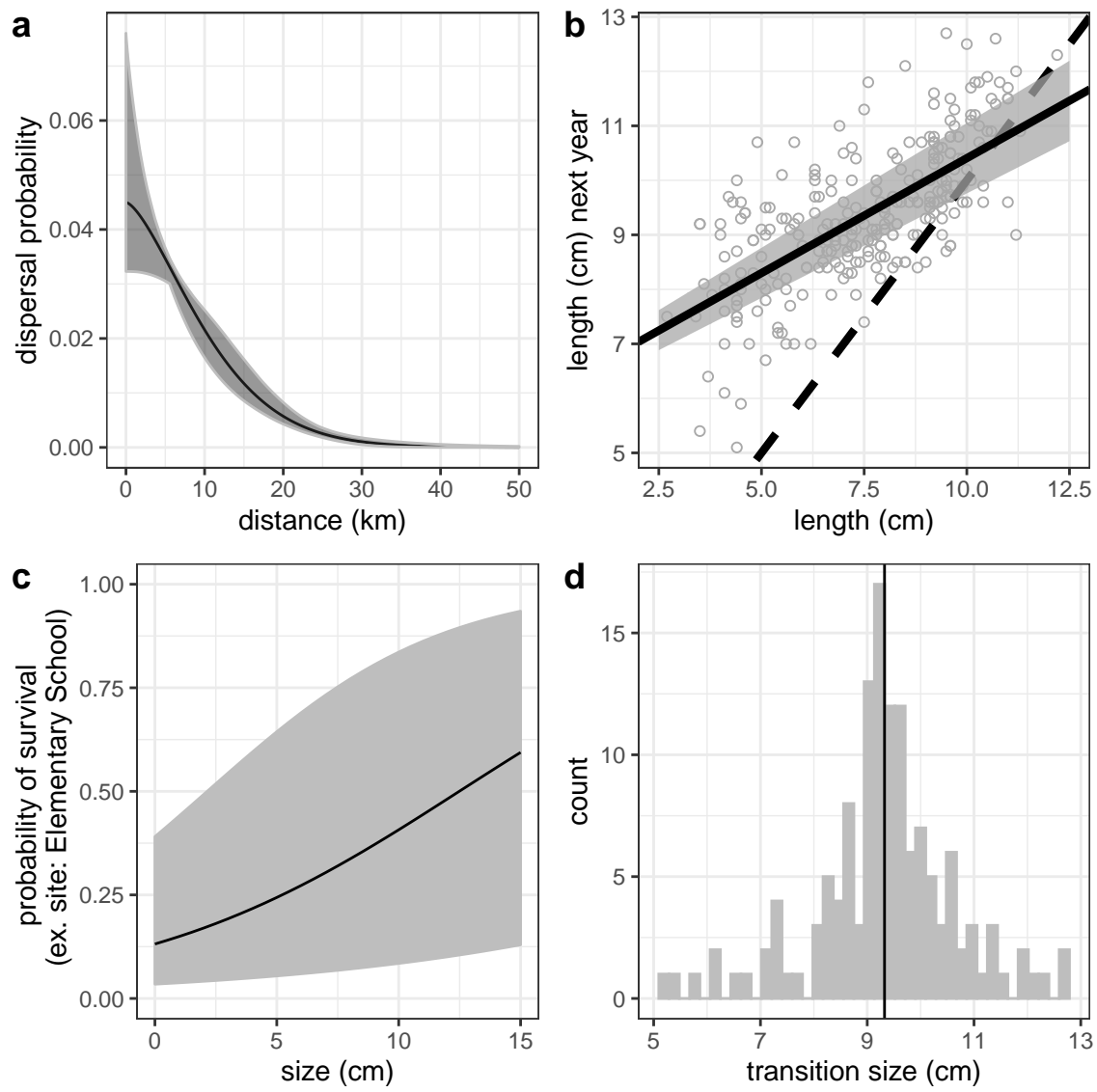


Figure 3: Best estimates (solid black line) and uncertainty (grey) for a) dispersal, b), growth, including the 1:1 line in thick black, c) post-recruit annual survival at Palanas as an example patch, and d) size at female transition parameters.

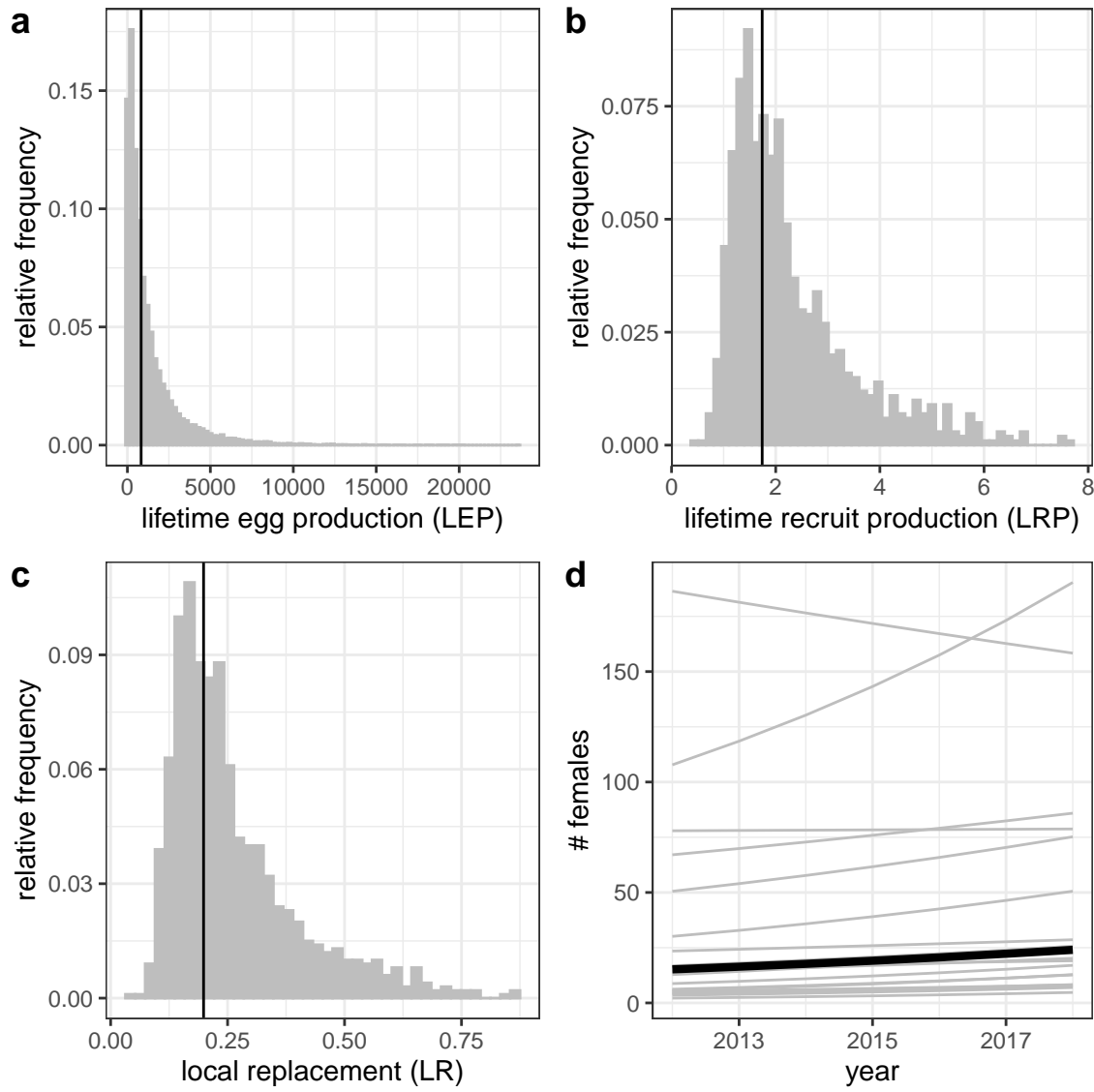


Figure 4: Estimates of a) estimated abundance of females over time at each individual patch (grey lines) and for an average patch (black line), b) individual-patch LEP_i for all patches with the best estimate averaged across patches (black line), c) average LRP across patches, and d) local replacement, showing the best estimate (black solid line) and range of estimates considering uncertainty in the inputs (grey). Estimates of LRP and LR include compensation for density-dependent mortality in early life stages.

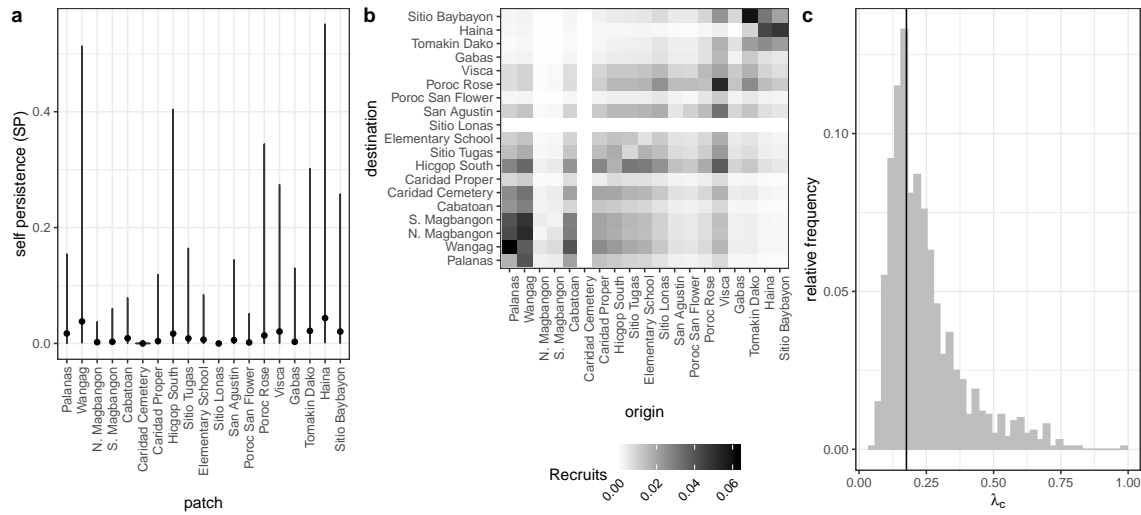


Figure 5: Values of a) self-persistence, b) realized connectivity among patches, and c) network persistence. All estimates include compensation for density-dependence in early life stages. For self-persistence (a) and network persistence (c), the best estimate is shown with in black (point for (a), line for (c)) and the range of estimates considering uncertainty is shown in grey.

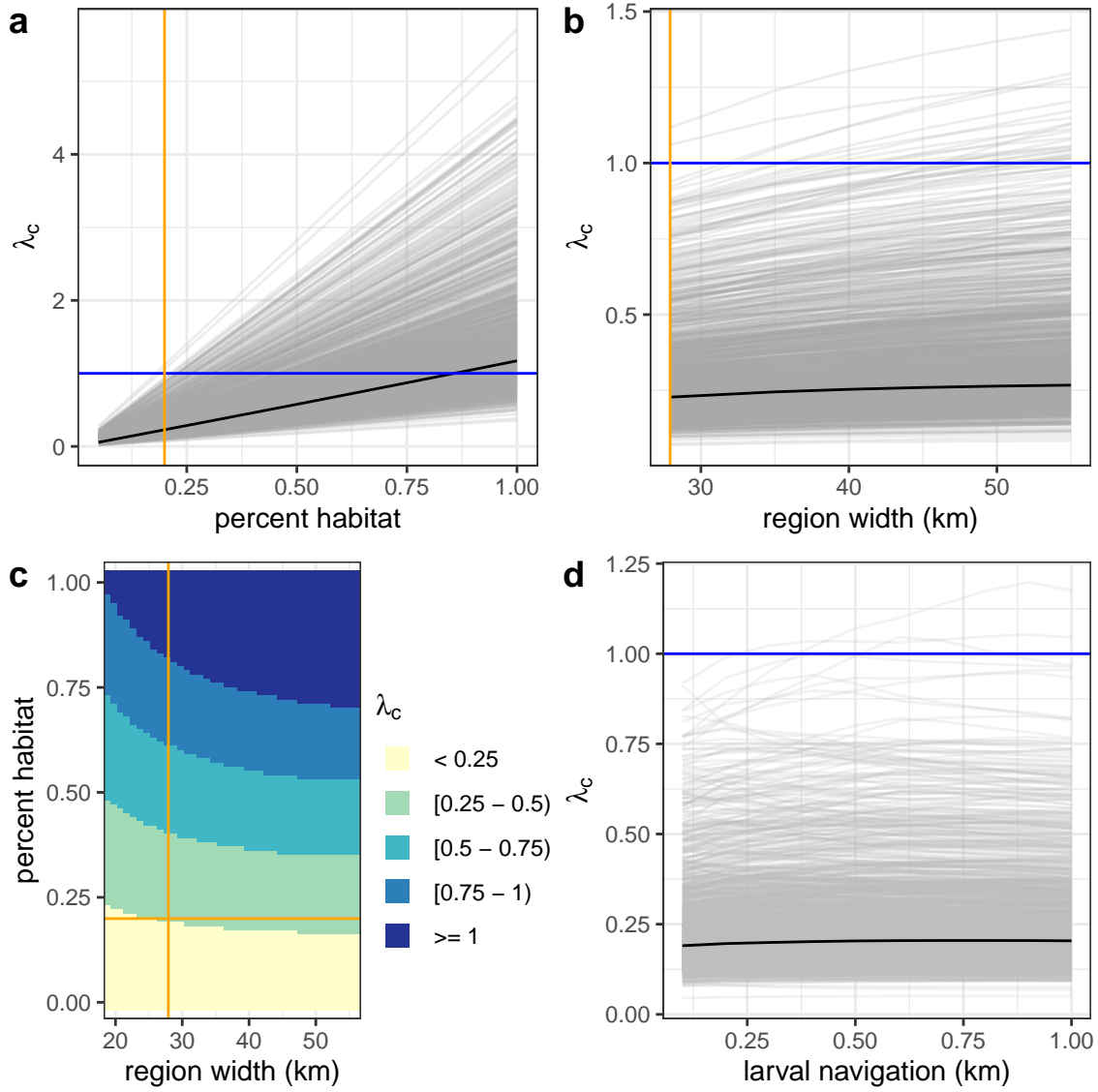


Figure 6: Sensitivity of network persistence to a) the proportion of the sampling region that is habitat, b) the width of the region maintaining the same proportion habitat (20%), c) the width of the region when 100% of the region is habitat, and d) larval navigation, where a buffer is added to the patch edges. Each metric calculation is a grey line and the best estimate is in black. The orange line shows the real proportion habitat and the blue line shows the persistence threshold.

Appendix

A Supplemental Methods

A.1 Defining recruit and census stage

When assessing persistence, we must consider mortality and reproduction that occurs across the entire life cycle to determine whether an individual is replacing itself with an individual that reaches the same life stage (Burgess et al., 2014). We defined a recruit to be a juvenile individual that has settled on the reef within the previous year, which also encompasses the size we were first able to sample (3.5-6.0 cm for parentage studies) (Fig. D.1). In theory, it does not matter how we defined recruit as long as we used that definition in our calculations of both egg-recruit survival and LEP. In our system, however, while it is straightforward to calculate LEP from any size, we did not have enough tagged recruits to reliably estimate survival to different recruit sizes. Instead, we chose the mean size of offspring matched in the parentage study as our best estimate of the size of a recruit ($\text{size}_{\text{recruit}}$) and tested sensitivity to different recruit sizes by sampling from a uniform distribution over the sizes the recruit stage covers (3.5-6 cm, Table A1).

A.2 Self persistence

Our equation for SP is a modification of that used in Burgess et al. (2014), which uses LEP to represent offspring produced and uses local retention (the number of surviving recruits that disperse back to the natal patch divided by the number of eggs

produced by the natal patch) to capture egg-recruit survival and dispersal combined: LEPlocal retention 1. We modify this to include egg-recruit survival in the offspring term instead, using LRP in place of LEP.

A.3 Dispersal kernel

A.4 Growth and survival

To include size in the mark-recapture model for survival, we used the growth model (eqn. 6) and the size recorded or estimated in the previous year to estimate the size of fish not recaptured in a particular year. Fish are not well-mixed at our patches and divers needed to swim near an anemone to have a reasonable chance of capturing the fish on it so we also included a distance effect on recapture probability (Table A3). We used diver GPS tracks to estimate the minimum distance between a diver and the anemone where the fish was first caught for each tagged fish in each sample year.

We compared the fit of the models using a modified version of the Akaike information criterion that reduces the potential for overfitting with small sample sizes (AICc) and selected the model with the lowest AICc value (Table A3).

A.5 Fecundity

We used a size-dependent fecundity relationship determined using photos of egg clutches and females (Yawdoszyn, in prep), where the number of eggs per clutch (E_c) is exponentially related to the length in cm of the female (L) with size effect $\beta_l = 2.388$, intercept $b = 1.174$, and egg age effect $\beta_e = -0.608$ dependent on if the

eggs were old enough to have visible eyes. For fish larger or equal to the transition to female size L_f , we multiplied the number of eyed eggs per clutch by the number of clutches per year $c_e = 11.9$ (estimate from Holtswarth et al., 2017) to get total annual fecundity f for a female of length L :

$$f(L) = \begin{cases} 0, & \text{if } L < L_f \\ c_e * e^{\beta_l \ln(L) + \beta_e [\text{eyed}] + b}, & L \geq L_f. \end{cases} \quad (\text{A.1})$$

A.6 Lifetime egg production (LEP)

To compute LEP, we discretized time and size (in eqn. 7) and summed across the matrix. When entering the starting individual into the matrix, we used 0.1 as the standard deviation of size to spread out the starting individual across size bins. To account for differences in growth rates across fish, we used the size determined by the growth curve (eqn. 6) as the mean along with an estimate of spread (size_{sd}) when projecting the size distribution of the fish in the next year. We used our recapture data to estimate the standard deviation (size_{sd}) of the distribution of sizes in the next year of fish starting from one size (Table A1).

LEP was estimated by site because each patch has a different estimate of survival, represented as LEP_i . We also present the average LEP across patches, noted as LEP_* (Fig. 4b) and used to estimate average LRP and LR for the metapopulation (Fig. 4c, d).

To estimate egg-recruit survival (S_e), we used the expected lifetime egg production for a fish that has already survived to reach parent size (6.0 cm) so L_s in eqn. 7

$= 6.0$, rather than 3.5 . We used the average LEP for parent-sized fish across patches, noted as LEP_p .

A.7 Alternate geographies and larval navigation

A.7.0.1 Larval navigation

In our sensitivity test to larval navigation and swimming, we added a buffer representing navigation ranging from $0 - 1$ km to the edges of the destination patches when determining probability of dispersal between patches. To avoid the shadows of effective patch area from overlapping, we added no more than half the distance between two adjacent patches to each patch. The buffers changed the proportion of the sampling region that is habitat (A.8.0.4), as we considered the buffer areas to be habitat as well, which affected the scaling of recruits in egg-recruit survival.

A.8 Scaling up recruits

To estimate the total number of offspring produced by genotyped parents that survived to recruitment, we scaled up the number of matched offspring caught during sampling (R_m) to account for recruits we could have missed (Fig. D.2). We scaled up by 1) the cumulative proportion of habitat we sampled at our patches over time (P_h) to account for recruits at anemones we did not sample (details in A.8.0.1), 2) the probability of capturing a fish if we sampled its anemone (P_c) to account for fish that escaped during sampling (details in A.8.0.2), 3) the proportion of the dispersal kernel from our patches covered within our sampling region (P_d) to account for fish that dispersed outside of our sampling area (details in A.8.0.3), and 4) the

proportion of our sampling region that was habitat (P_s) to avoid counting mortality of fish dispersing to non-habitat within our region twice (in both the estimate of total recruits and in the integrated dispersal kernel) (details in A.8.0.4).

A.8.0.1 Proportion of habitat sampled

We used tagged anemones to estimate the proportion of habitat we sampled within our patches. We tagged each anemone that was home to yellowtail anemonefish with a metal tag, which is relatively permanent and easy to re-sight (the anemone tag is visible above the anemone in Fig. 2c). We therefore considered the total number of metal-tagged anemones at a patch to be the habitat present. We used proportion of anemones rather than proportion of total patch area because anemones, and therefore habitat quality, were unevenly distributed across each patch; areas we did not visit likely had a lower anemone density than the areas we did sample.

To scale the number of tagged recruited offspring to account for areas of our patches we did not sample, we used the overall proportion habitat sampled across all patches and sampling years (P_h). We summed the metal-tagged anemones we visited across all patches and years, then divided by the number of anemones we could have sampled (the sum of total metal-tagged anemones across all patches multiplied by the number of sampling years).

A.8.0.2 Probability of capturing a fish, from recapture dives

To estimate the probability of capturing a fish given that we sampled its anemone (P_c), we used mark-recapture data from recapture dives done within a sampling

season. During some of the sampling years, portions of the patches were sampled again within a few weeks of the original sampling dives. We assumed that the probability of recapturing a fish on a recapture dive was the same as capturing a fish on a sampling dive, assuming there was no mortality in the weeks between dives and that the fish did not alter their behavior towards divers. For each recapture dive, we used GPS tracks of the divers to identify the anemones covered in the recapture dive and the set of PIT-tagged fish encountered on those anemones during the original sampling dives. We estimated the probability of capture P_c as the number of tagged fish re-caught during the capture dive m_2 divided by the total number of fish caught on the recapture dive n_2 : $P_c = \frac{m_2}{n_2}$.

We used the mean P_c across all 14 recapture dives, covering XX patches in 3 sampling seasons (2016, 2017, 2018), as our best estimate. To consider uncertainty in P_c , we represented the probability of capture as a beta distribution, using the mean μ_{P_c} and variance V_{P_c} of the set of 14 values to find the appropriate α_{P_c} and β_{P_c} parameters, where

$$\alpha_{P_c} = \left(\frac{1 - \mu_{P_c}}{V_{P_c}} - \frac{1}{\mu_{P_c}} \right) \mu_{P_c}^2 \quad (\text{A.2})$$

$$\beta_{P_c} = \alpha_{\mu_{P_c}} \times \frac{1}{\mu_{P_c} - 1}. \quad (\text{A.3})$$

The mean of the individual capture probability values was $\mu_{P_c} = 0.56$, with variance $V_{P_c} = 0.069$, giving beta distribution parameters $\alpha_{P_c} = 1.44$ and $\beta_{P_c} = 1.13$. We sampled 1000 values from the beta distribution, then truncated the sample to

include only values larger than the lowest value of P_c estimated from an individual dive (0.20), to avoid unrealistically low values randomly sampled from the distribution. We then sampled with replacement from the truncated set to get a vector of 1000 values.

A.8.0.3 Proportion of dispersal kernel area sampled

To account for recruits that dispersed outside our sampling region, we found the proportion of the dispersal kernels from all parents that fell within our sampling region. For each of the nineteen patches, we found the area under the kernel (A_i) from the center of the patch to the north edge of the sampling area (d_N) (northern-most tagged anemone at Palanas, the northern-most patch) and the center of the patch to the south edge of the sampling area (d_S) (southern-most tagged anemone at Sitio Baybayon, the southern-most patch), then multiplied by the number of genotyped parents at that patch (N_{g_i}). We added the areas together, then divided by the sum of the total area under the dispersal kernel in both directions (1 when the kernel was normalized to 0.5) multiplied by the total number of genotyped parents (N_g) to get the proportion of the total dispersal kernel area covered by our sampling region (P_d):

$$A_i = N_{g_i} \left(\int_0^{d_N} z e^{-(zd)^{\theta}} dd + \int_0^{d_S} z e^{-(zd)^{\theta}} dd \right), \quad (\text{A.4})$$

$$P_d = \frac{\sum_{i=1}^{19} A_i}{N_g}. \quad (\text{A.5})$$

A.8.0.4 Proportion habitat in sampling area

To avoid counting mortality due to larvae settling on non-habitat twice - once in scaling up our matched recruits, which only included those who settled on habitat, and once in integrating the dispersal kernel - we scaled the estimate of total surviving recruits from our patches by the proportion of our sampling region that was habitat (P_s). We found P_s by summing the lengths of all the patches, which run approximately north-south, and dividing by the total north-south distance of our sampling region, giving $P_s = 0.20$. We assumed that larvae were unable to navigate to habitat if they dispersed to an unsuitable area but relaxed that assumption in our sensitivity tests (A.7.0.1) as anemonefish larvae do likely have some ability both to sense good settlement areas, either by detecting host anemones (Elliott et al., 1995; Arvedlund et al., 1999) or conspecifics (e.g. Lecchini et al., 2005, for coral reef fish more broadly), and to swim in a particular direction (e.g. Bellwood and Fisher, 2001; Fisher, 2005).

A.9 Characterizing uncertainty

A.9.0.1 Dispersal kernel

To account for uncertainty in the dispersal kernel, we used sets of the shape parameter θ and the scale parameter k_d that represented the span of the 95% confidence interval when k_d and θ were estimated jointly (Table A1, Catalano et al., in prep). We randomly sampled pairs of θ and k_d parameters from the distribution, weighted by the log-likelihood.

A.9.0.2 Growth

We used the first and second capture lengths for fish that were recaptured after a year (within 345 to 385 days) to estimate L and K (using eqn. 6). For fish recaptured more than once, we randomly selected only one recapture period from each to use to estimate the von Bertalanffy parameters and repeated the random selection and estimate 1000 times. We found the mean estimates ($L = 10.70$ cm, $K = 0.864$) and mean standard error of those fits, then sampled from within that range to generate a set of von Bertalanffy growth curves to use in our LEP calculations (Fig. 2b, Table A1).

A.9.0.3 Survival

A.9.0.4 Size of transition to female

To incorporate uncertainty in the size at which male fish transition to female (and reproductive output is counted in eqn. 7), we sampled directly from the sizes at which recaptured fish were first captured as female (5.2 cm - 12.7 cm) (Fig. 3d).

A.9.0.5 Lifetime Egg Production (LEP)

A.9.0.6 Egg-recruit survival

We considered uncertainty in the number of offspring assigned to parents (R_m) and in the probability of capturing a fish (P_c). We generated a set of values for the number of assigned offspring using a random binomial, with the number of genotyped offspring (745) as the number of trials and the assignment rate from the parentage

analysis (0.079) as the probability of success on each trial (Catalano et al., in prep). For the probability of capturing a fish, we sampled values from a beta distribution that captured the mean and variance of capture probabilities across recapture dives (details in A.3).

B Supplemental Results

B.1 Parentage

From the genetic work and parentage analysis done in Catalano et al. (in prep), we genotyped 1729 potential parents, genotyped 791 potential offspring, and matched 71 offspring to parents.

B.2 Growth

From the mark-recapture analysis of tagged and genotyped fish, we estimated mean values of $L_\infty = 10.70$ cm (with uncertainty bounds 9.81-11.65) and $K = 0.864$ (0.80-0.91) for the von Bertalanffy growth curve parameters (eqn. 6, Fig. 3b, Table A1).

B.3 Survival

The best model for post-recruitment annual survival ϕ on a log-odds scale had a positive size effect ($b_a = 0.15 \pm 0.029$ SE) with intercepts b_{ϕ_i} varying by patch (eqn. B.1, Fig. D.5). The accompanying best model for recapture probability p_r on a log-odds scale had a negative effect of size ($b_1 = -0.16 \pm 0.09$ SE) and a negative effect of diver distance from anemone ($b_2 = -0.15 \pm 0.02$ SE), with intercept $b_{p_r} = 2.14 \pm 0.87$ SE (eqn. B.2, Fig. D.6). This suggests divers were less likely to recapture larger fish, which are stronger swimmers and more likely to flee when divers approach, and those at anemones far from areas sampled:

$$\log\left(\frac{\phi}{1-\phi}\right) = b_{\phi_i} + b_a \text{size}. \quad (\text{B.1})$$

$$\log\left(\frac{p_r}{1-p_r}\right) = b_{p_r} + b_1 \text{size} + b_2 d. \quad (\text{B.2})$$

B.4 Lifetime egg production (LEP)

We calculated an average value of LEP across patches of 721 eggs with uncertainty bounds [82, 31657] (Fig. 4b), with best estimate values at individual patches that ranged from 0 to 1754 eggs. Uncertainty in adult survival had the largest effect on LEP (Fig. D.11), which corresponds to longer-surviving individuals having more opportunities to reproduce at larger sizes.

B.5 Egg-recruit survival (S_e)

We estimated egg-recruit survival S_e to be 0.002 [3.5e-05, 0.014] when we corrected for density-dependence in our data. Uncertainty in the size of transition to breeding female L_f had the largest effect on egg-recruit survival (Fig. D.13); the larger the transition size to female, the fewer tagged eggs we estimated were produced by our genotyped parents and the higher the estimate of egg-recruit survival. This differs from our finding above that adult survival had the largest effect on LEP because the starting size of the individual considered is lower when we estimate LEP for a recruit (4.37 cm, 3.5-6.0cm range) than for a parent (6.0cm). Fish considered parents in our parentage analysis have already survived one or more years since recruiting so the

transition to breeding female plays a larger role in the number of eggs they are likely to produce than for fish who have just recruited.

B.6 Abundance trends by patch

We used the number of females captured at each patch in each sampling year, scaled by the proportion of habitat sampled at that patch in that year and by the probability of capturing a fish, to estimate abundance trends for each patch (Fig. D.7). Seventeen of the patches showed positive abundance trends (Fig. D.7a-q), while the two southern-most patches showed declines (Haina and Sitio Baybayon, Fig. D.7r,s).

B.7 Persistence metrics without compensation for density-dependence

Estimating persistence metrics without compensating for density-dependence in our data gave us an understanding of whether individuals at our patches were able to replace themselves and whether our patches would persist in isolation at the current abundance levels, rather than at low abundance. Without compensation for early life density-dependence, all of our metrics showed that the set of patches we sampled is less likely to persist as an isolated network than the metrics for low abundance. We estimated egg-recruit survival (S_e) to be 0.0012 with uncertainty bounds [2.04e-05, 0.008] and average lifetime recruit production (LRP) across patches to be 0.84 [0.36, 4.54], with 55% of LRP estimates ≥ 1 . (Fig. D.9c). Our estimate of local replacement (LR), which estimates replacement for recruits from our patches returning to our patches implicitly including dispersal, was 0.10 [0.04, 0.52].

When we calculated LR using all arriving recruits to our patches, however, rather than just those originating there, the best estimate was > 1 (1.22, with 89% of values with uncertainty ≥ 1), suggesting that there was recruit-recruit replacement at our patches when we included immigrant recruits, even at current population levels when density-dependence was present.

We did not find any patches with a best estimate of $SP \geq 1$ or with uncertainty bounds that reached or exceeded 1 (Figs. D.10a). Our best estimate of the dominant eigenvalue of the realized connectivity matrix λ_c was 0.09 [0.04, 0.90] with 0% of estimates where $\lambda \geq 1$ (Fig. D.10c).

C Supplemental Tables

Table A1: Summary of parameter symbols, definitions, and values, including sections and equations where each are described in detail.

Parameter	Description	Best estimate [uncertainty bounds]	Uncertainty origin	Details	Notes
<i>Dispersal and demographics</i>					
K_d	scale parameter in dispersal kernel	XX	drawn from joint 95% confidence limits with θ , weighted by log-likelihood	eqn. 5	estimated in Cata-lano et al. (in prep) using methods in Bode et al. (2018)
θ	shape parameter in dispersal kernel	XX	drawn from joint 95% confidence limits with k_d , weighted by log-likelihood	eqn. 5	estimated in Cata-lano et al. (in prep) using methods in Bode et al. (2018)
L_∞	average asymptotic size (cm) in von Bertalanffy growth curve	10.70 cm []	growth curve estimated with different pairs of fish	eqn. 6	
k	growth coefficient in von Bertalanffy growth curve	0.864 []	XX	eqn. 6	
<i>Habitat and region characteristics</i>					
<i>Alternate geographies and scenarios</i>					

Table A2: Table with site-specific survival (ϕ_i) values on a log-odds scale (used in eqn. B.1), where the intercept is for adult survival for a fish of size 0 cm. The intercepts for each site is the intercept for Cabatoan plus the additional intercept value for that site, shown in the table.

Site	Intercept	Standard error	Confidence limits	Notes
Cabatoan	-1.78	0.33	-2.42 to -1.14	
Caridad Cemetery	-19.66	0.00	-19.66 to -19.66	addition to Cabatoan intercept
Elementary School	-0.11	0.41	-0.92 to 0.69	addition to Cabatoan intercept
Gabas	-0.42	0.58	-1.55 to 0.72	addition to Cabatoan intercept
Haina	0.12	0.35	-0.57 to 0.81	addition to Cabatoan intercept
Higcop South	-0.06	0.46	-0.96 to 0.84	addition to Cabatoan intercept
N. Magbangon	-1.31	0.38	-2.05 to -0.57	addition to Cabatoan intercept
Palanas	0.24	0.26	-0.26 to 0.75	addition to Cabatoan intercept
Poroc Rose	-0.19	0.44	-1.05 to 0.68	addition to Cabatoan intercept
Poroc San Flower	-0.52	0.48	-1.45 to 0.42	addition to Cabatoan intercept
San Agustin	-0.47	0.50	-1.45 to 0.42	addition to Cabatoan intercept
Sitio Baybayon	0.02	0.26	-0.49 to 0.52	addition to Cabatoan intercept
S. Magbangon	-1.08	0.48	-2.02 to -0.14	addition to Cabatoan intercept
Tomakin Dako	0.39	0.33	-0.25 to 1.03	addition to Cabatoan intercept
Visca	0.33	0.35	-0.36 to 1.01	addition to Cabatoan intercept
Wangag	0.35	0.25	-0.15 to 0.85	addition to Cabatoan intercept

Table A3: Table showing the set of models considered in MARK for survival (ϕ) (from eqn. B.1) and recapture (p_r) (from eqn. B.2) probability, including effects of fish size (S), minimum distance from diver to the anemone where fish were first caught during surveys (D), year (t), and patch (i), and their relative AICc scores.

Model	Model description	AICc	dAICc
$\phi \sim S + i, p_r \sim S + D$	survival size+patch, recapture size+distance	3104.1	0
$\phi \sim i, p_r \sim S + D$	survival patch, recapture size+distance	3127.2	-23.1
$\phi \sim i, p_r \sim D$	survival patch, recapture distance	3127.2	-23.1
$\phi \sim S, p_r \sim S + D$	survival size, recapture size+distance	3139.9	-35.8
$\phi \sim S, p_r \sim D$	survival size, recapture distance	3141.6	-37.5
$\phi, p_r \sim S + D$	survival constant, recapture size+distance	3168.4	-64.3
$\phi, p_r \sim D$	survival constant, recapture distance	3169.3	-65.2
$\phi \sim t, p_r$	survival time, recapture constant	3243.9	-139.8
$\phi \sim i, p_r$	survival patch, recapture constant	3254.4	-150.3
$\phi, p_r \sim t$	survival constant, recapture time	3274.0	-169.9
$\phi \sim S, p_r \sim S$	survival size, recapture size	3345.1	-241.0
ϕ, p_r	survival constant, recapture constant	3382.7	-278.6

Table A4: Table showing the percent of anemones surveyed at each patch, ordered from north to south, in each sampling year.

		% Habitat surveyed						
Patch	# Total anems	2012	2013	2014	2015	2016	2017	2018
Palanas	138	29	57	48	61	85	86	86
Wangag	291	18	33	42	35	27	49	69
N. Magbangon	105	5	12	40	63	64	0	5
S. Magbangon	34	41	56	32	0	65	0	71
Cabatoan	26	42	58	58	65	73	0	62
Caridad Cemetery	4	0	75	50	0	50	50	50
Caridad Proper	4	0	100	0	0	0	0	0
Hicgop South	18	0	67	28	28	56	83	78
Sitio Tugas	8	0	100	0	0	0	0	0
Elementary School	7	0	100	43	100	100	86	100
Sitio Lonas	1	100	100	0	0	0	0	0
San Agustin	18	89	61	72	61	100	89	72
Poroc San Flower	11	100	82	73	73	55	82	64
Poroc Rose	13	100	100	69	31	23	69	69
Visca	13	100	100	23	38	62	85	62
Gabas	9	0	0	0	44	44	67	0
Tomakin Dako	48	0	25	23	38	35	60	69
Haina	104	0	6	13	13	10	56	80
Sitio Baybayon	259	0	14	30	34	30	41	81
Overall	1111	16	32	36	39	42	48	67

Table A5: Table showing patch-specific estimates of lifetime egg production (LEP_i), lifetime recruit production (LRP_i), and self persistence (SP_i .)

Patch	LEP_i	LRP_i	SP_i
Palanas	1383	2.91	0.017
Wangag	1642	3.45	0.040
N. Magbangon	133	0.28	0.002
S. Magbangon	183	0.39	0.003
Cabatoan	933	1.96	0.009
Caridad Cemetery	0	0	0
Caridad Proper	781	1.64	0.004
Hicgop South	848	1.78	0.017
Sitio Tugas	781	1.64	0.003
Elementary School	781	1.64	0.007
Sitio Lonas	781	1.64	0
San Agustin	445	0.92	0.006
Poroc San Flower	415	0.87	0.002
Poroc Rose	694	1.46	0.014
Visca	1586	3.34	0.021
Gabas	483	1.02	0.003
Tomakin Dako	1760	3.70	0.022
Haina	1130	2.38	0.044
Sitio Baybayon	959	2.02	0.021

D Supplemental Figures

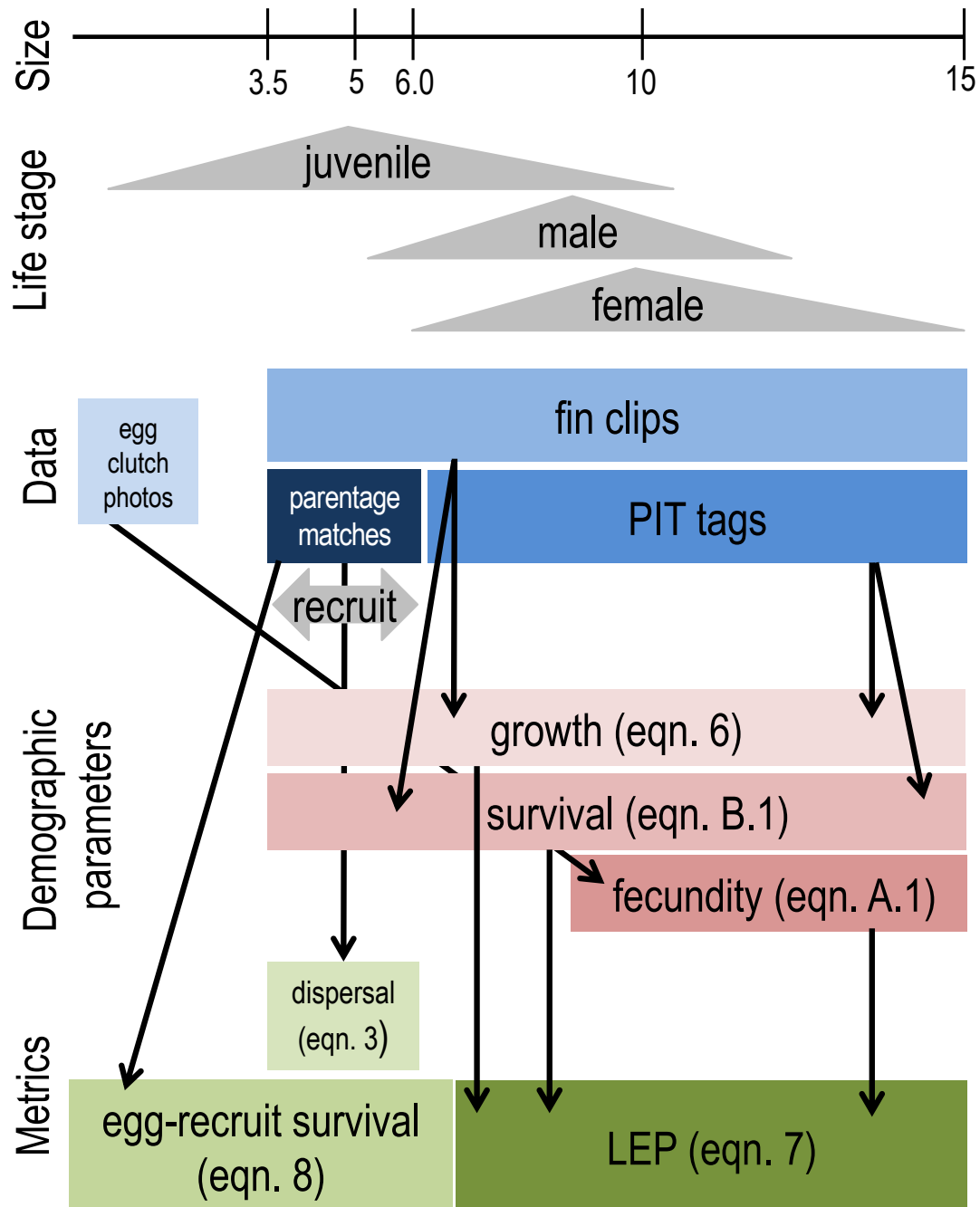


Figure D.1: The data collected for fish at each life stage and how they match to the equations and metrics estimated. We considered recruits to be offspring in their first year of settlement, represented by the 3.5–6.0 cm range.⁵⁴

How could we have missed potential recruits originating from our patches?

- 1) Failed to catch recruit when sampling (P_c)
- 2) Missed sampling some habitat areas within our patches (P_h)
- 3) Recruit dispersed outside our study region (P_d)
- 4) Recruit dispersed to non-habitat within our region (P_s)
- 5) Recruit died due to density-dependent competition with other settlers (DD)

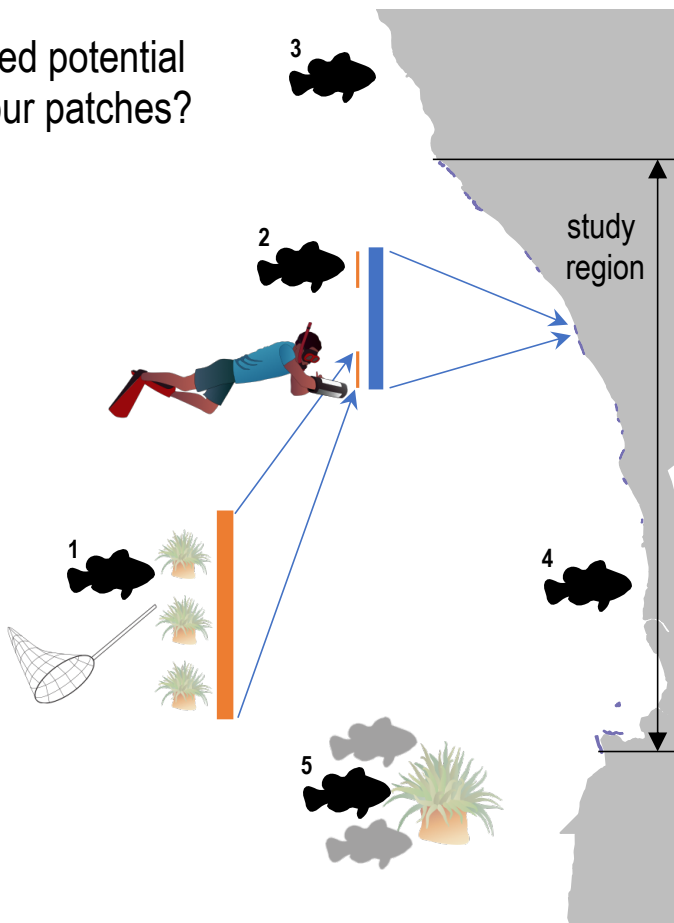


Figure D.2: Schematic of five ways we could have missed recruits while sampling and used to scale up our raw estimate of recruits from matched offspring.

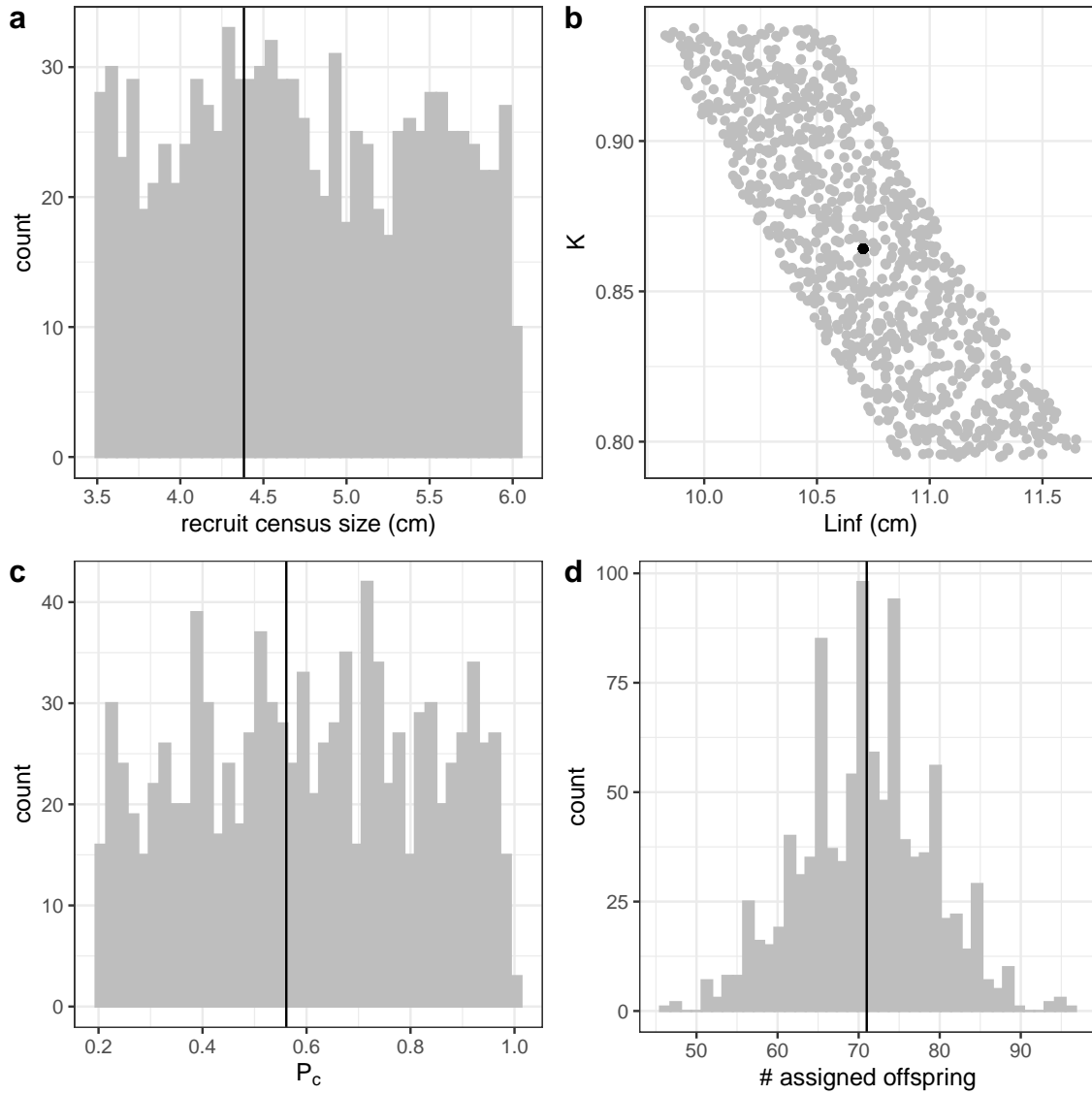


Figure D.3: Range of parameter inputs for uncertainty runs with all uncertainty included, where the black line or point is the value used for the best estimate: a) $\text{size}_{\text{recruit}}$, the census size for recruits after egg-recruit survival; b) the parameters L_∞ and K of the von Bertalanffy growth model; c) P_c , the probability of capturing a fish; d) number of offspring assigned back to parents in the parentage analysis; e) factors that scale the number of estimated recruits from our patch based on density-dependence in settler success (DD), proportion of the dispersal kernel captured by our sampling region (P_d), the cumulative proportion of our patches we sampled over time (P_h), and the proportion of our sampling area that was habitat (P_s).

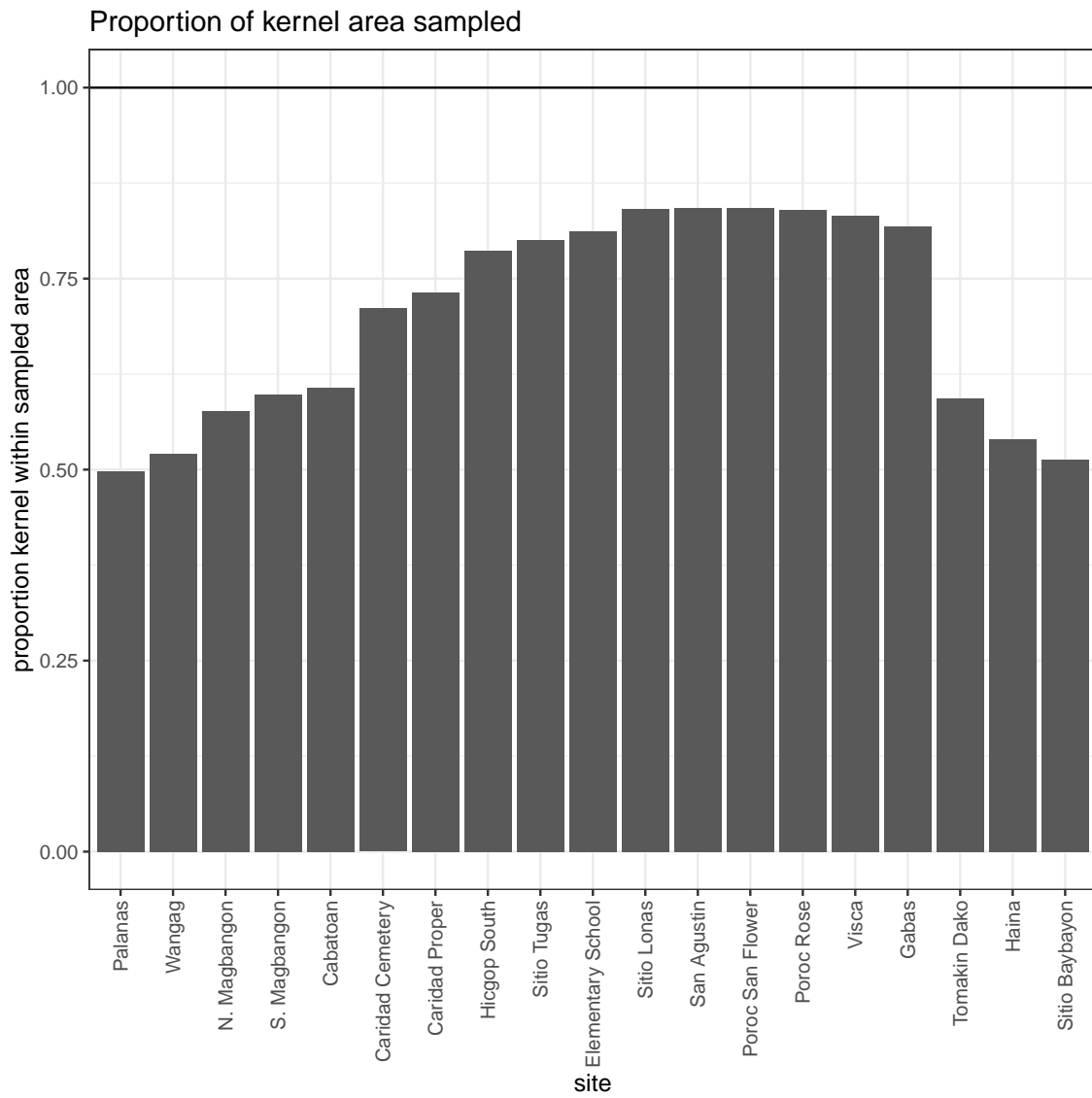


Figure D.4: Proportion of the dispersal kernel area from the center of each patch covered by our sampling region. The overall proportion (P_d) is weighted by the number of parents at each patch.

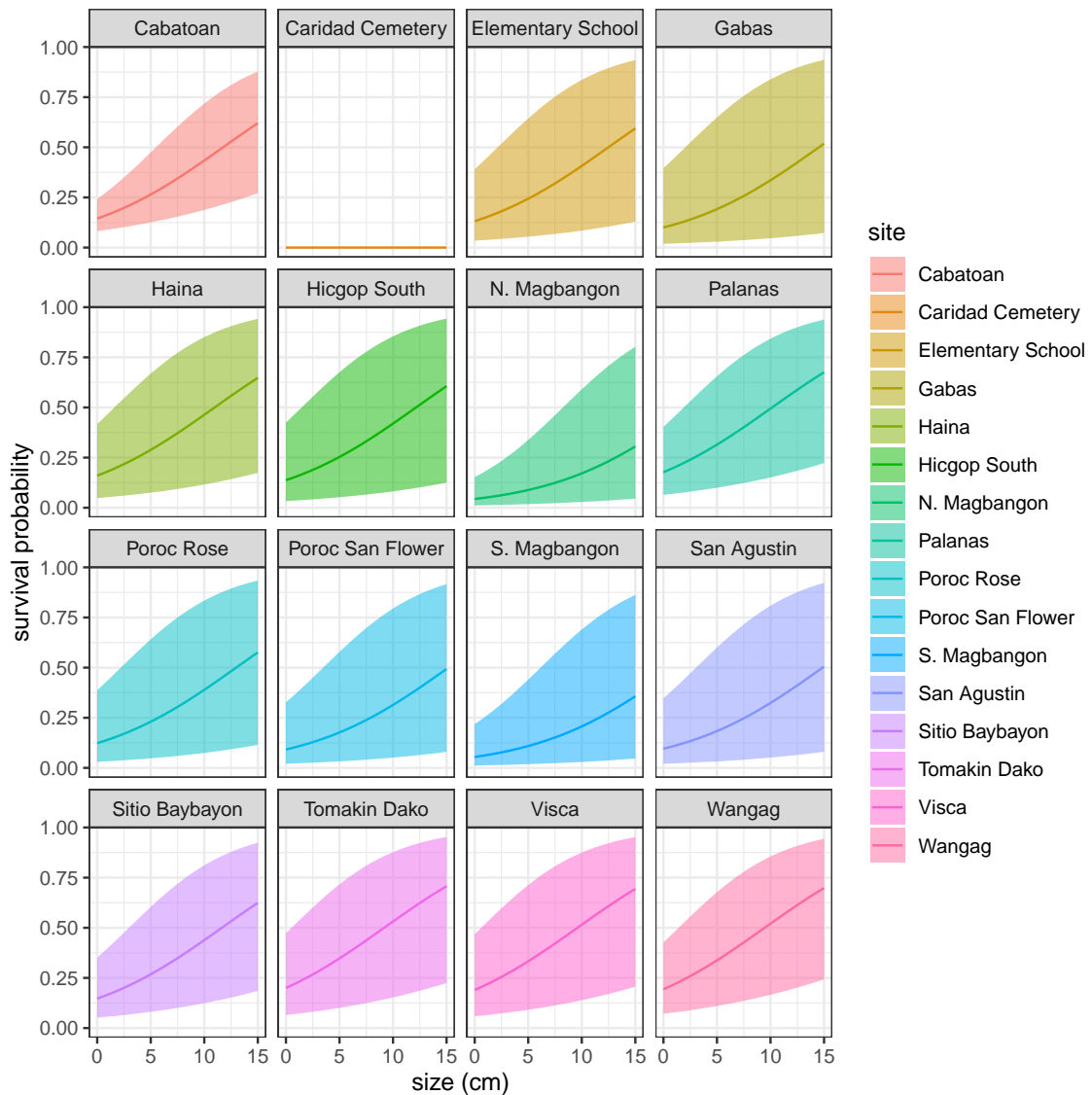


Figure D.5: Annual survival by size at each patch.

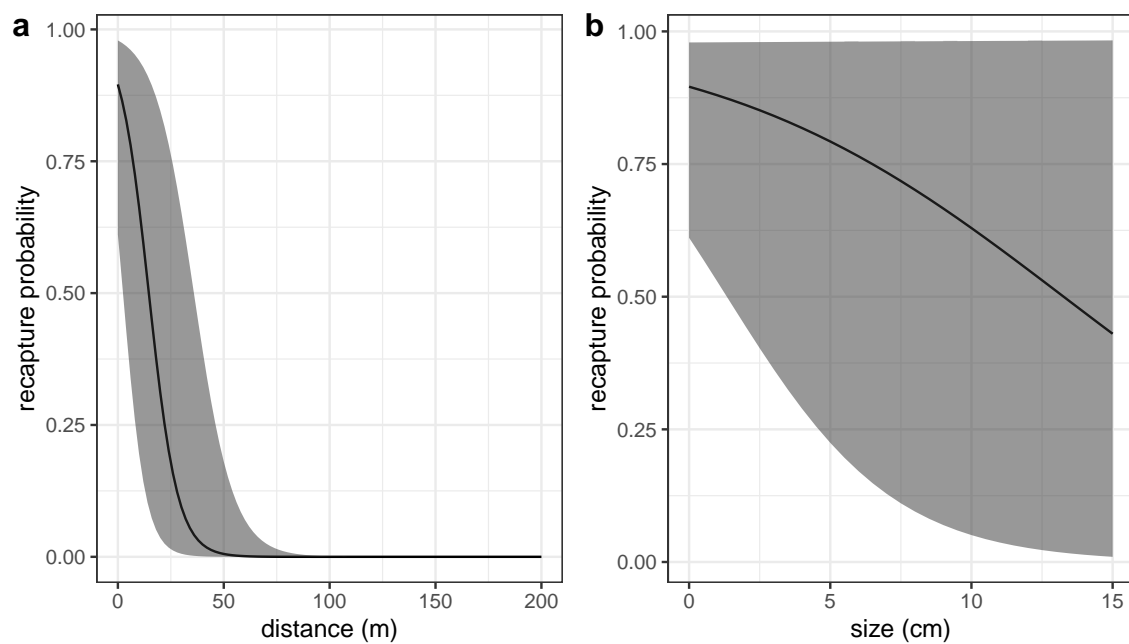


Figure D.6: Effects of a) minimum distance between divers and the anemone where the fish was first caught and b) fish size on recapture probability, estimated along with survival in a mark-recapture analysis.

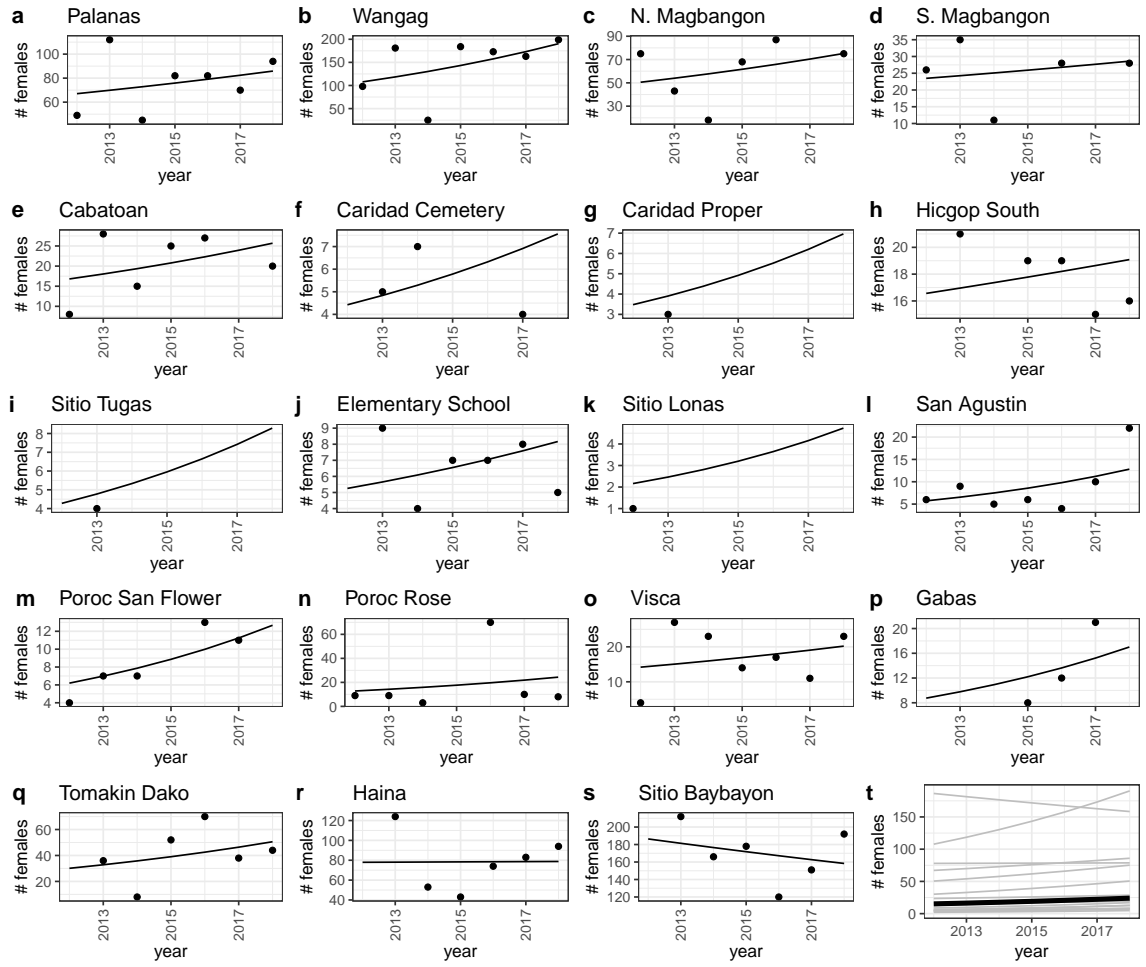


Figure D.7: Scaled number of females captured (black dots) and abundance trends (black lines) by patch from a mixed effects model with patch as a random effect.

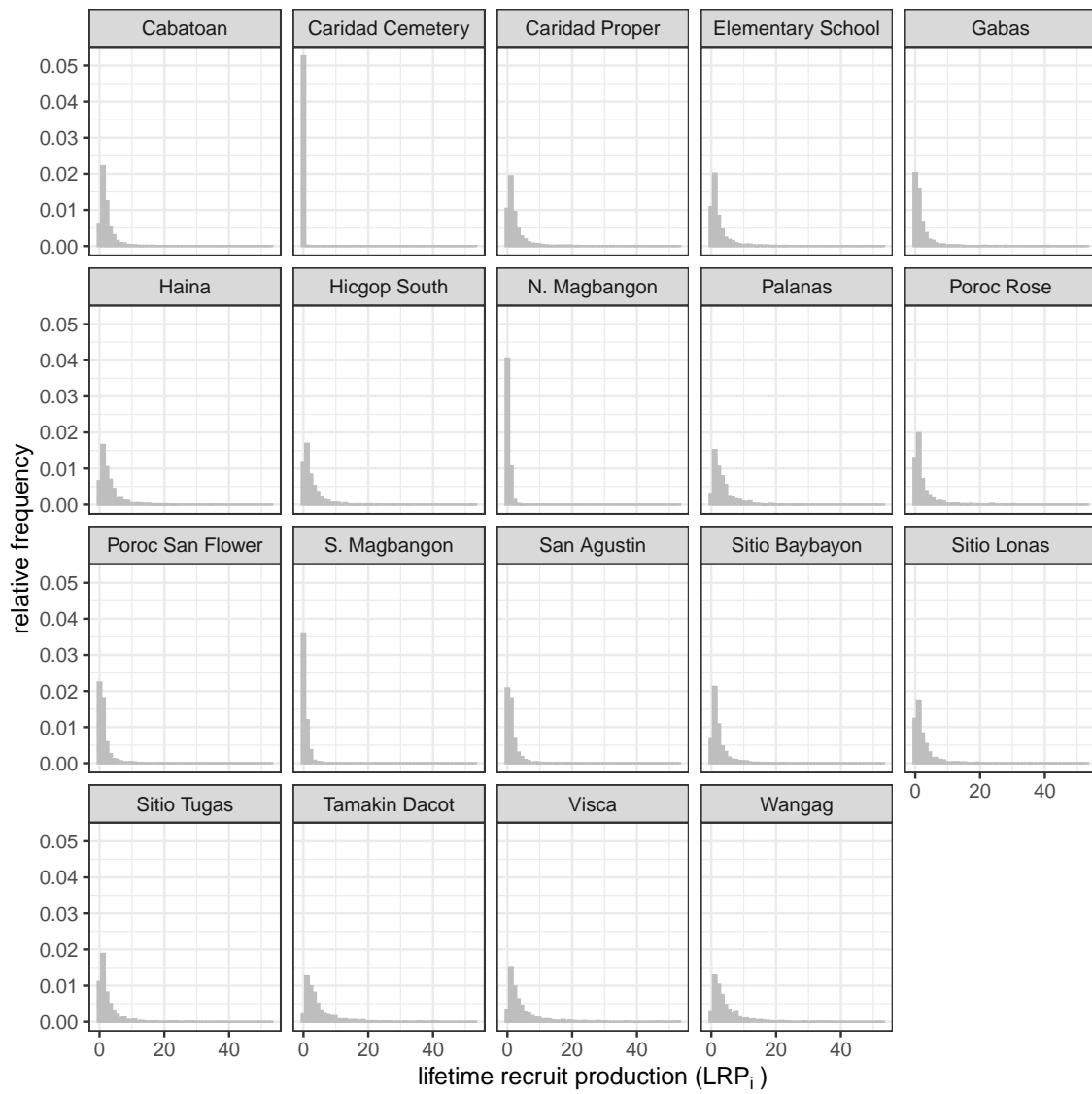


Figure D.8: Site-specific lifetime recruit production (LRP_i) estimates.

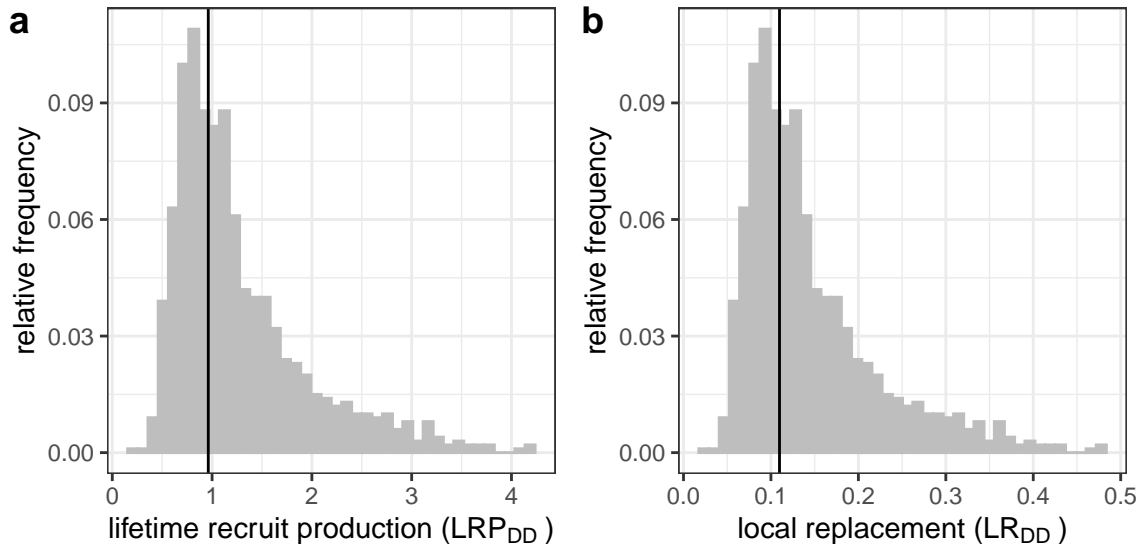


Figure D.9: Estimates of a) LRP, and b) local replacement without compensating for density dependence in early life stages in our data, showing the best estimate (black solid line) and range of estimates considering uncertainty (grey) in the inputs. These estimates compare to those in 4c,d, where we corrected for additional mortality in early life due to density dependence.

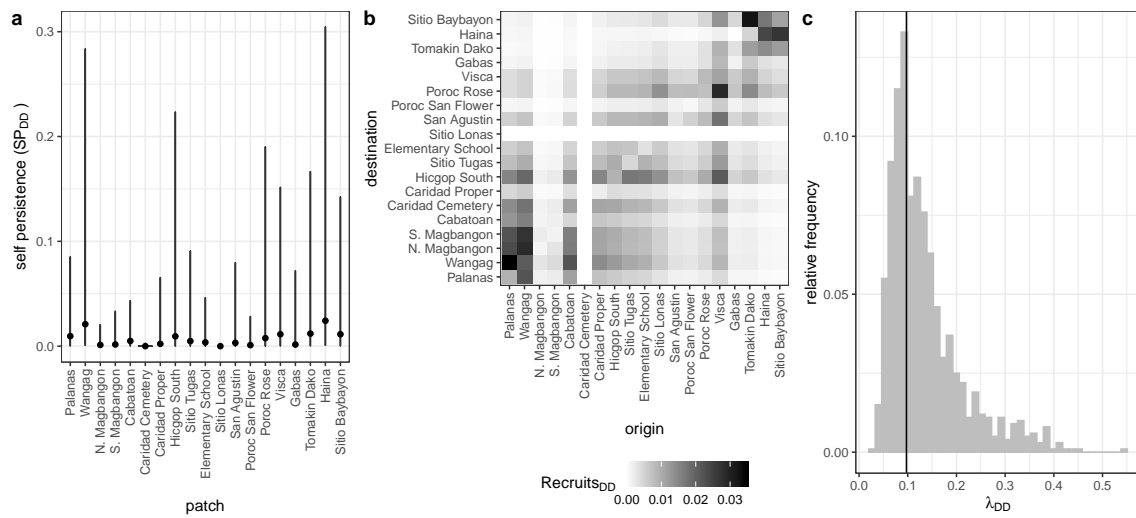


Figure D.10: Values of a) self-persistence, b) realized connectivity among patches, and c) network persistence without compensation for density-dependence in early life stages in our data. For self-persistence (a) and network persistence (c), the best estimate is shown with in black (point for (a), line for (c)) and the range of estimates considering uncertainty is shown in grey. These estimates compare to those in 5 where we compensated for density dependence in early life stages.

Here we show the contribution of uncertainty of each input to the overall uncertainty in the values of LEP (Fig. D.11), LRP (Fig. D.12), egg-recruit survival S_e (Fig. D.13), and network persistence λ_c (Fig. D.14). We calculated the metrics using best estimates for all inputs except the one shown and show the results as violin plots, which show vertical probability densities of the metrics across a range of values.

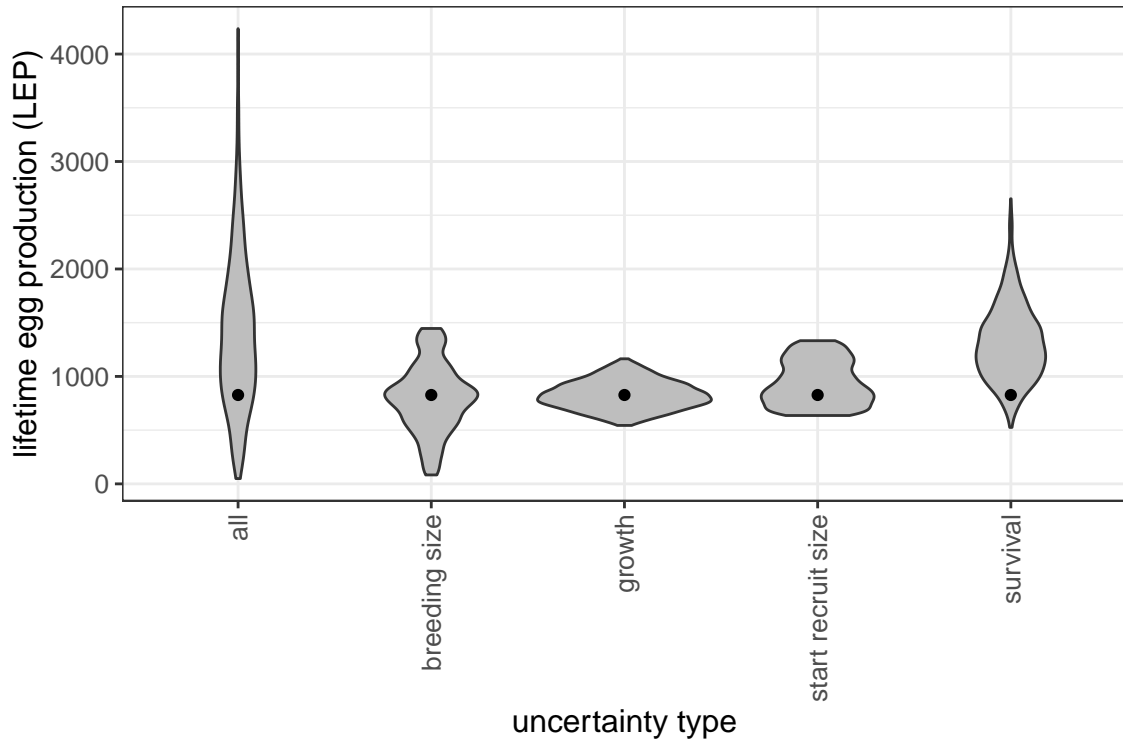


Figure D.11: The contribution of different sources of uncertainty in LEP.

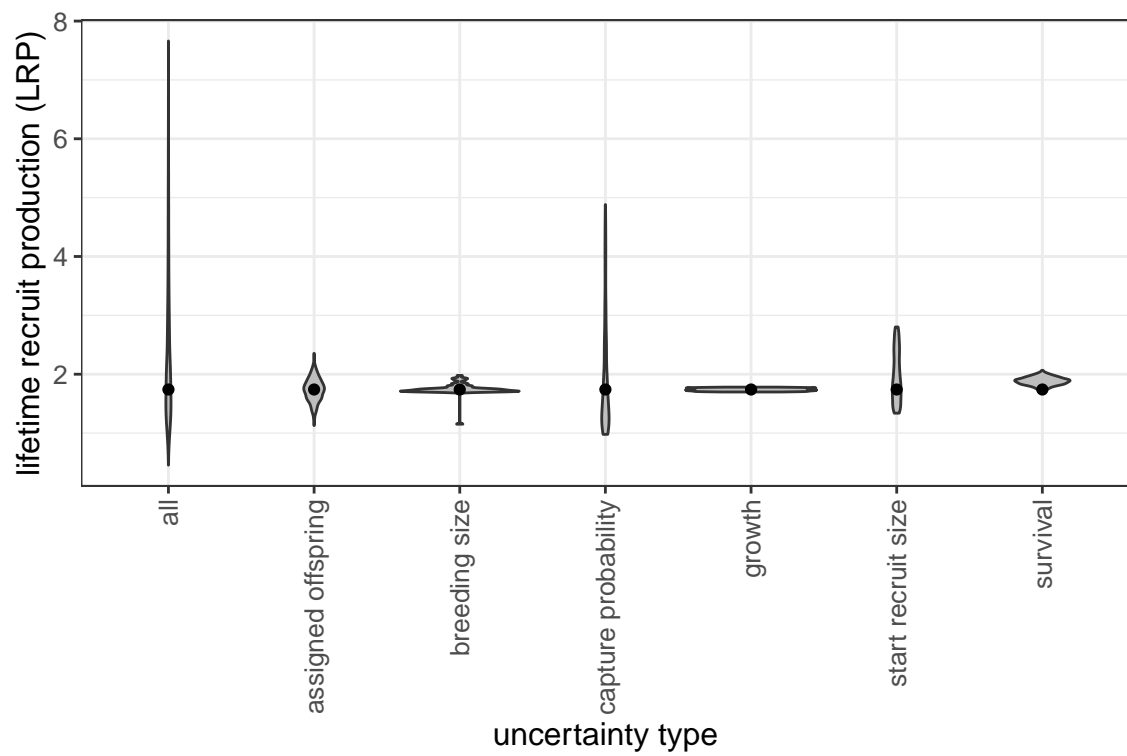


Figure D.12: The contribution of different sources of uncertainty in LRP.

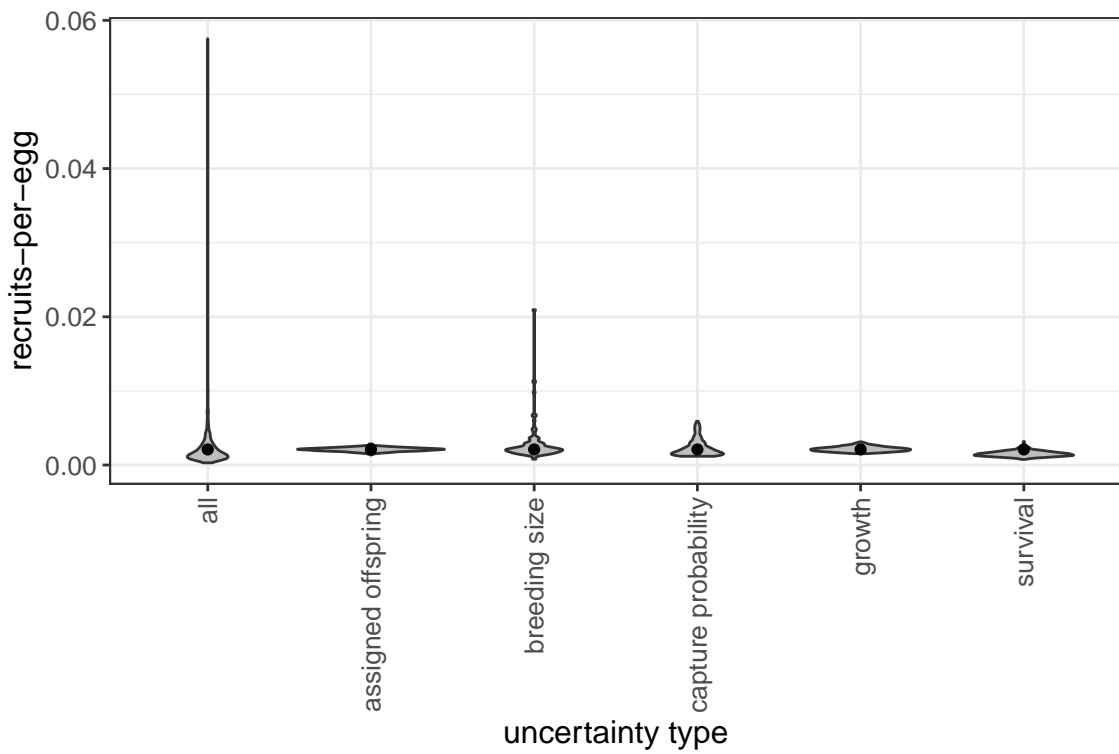


Figure D.13: The contribution of different sources of uncertainty in egg-recruit survival.

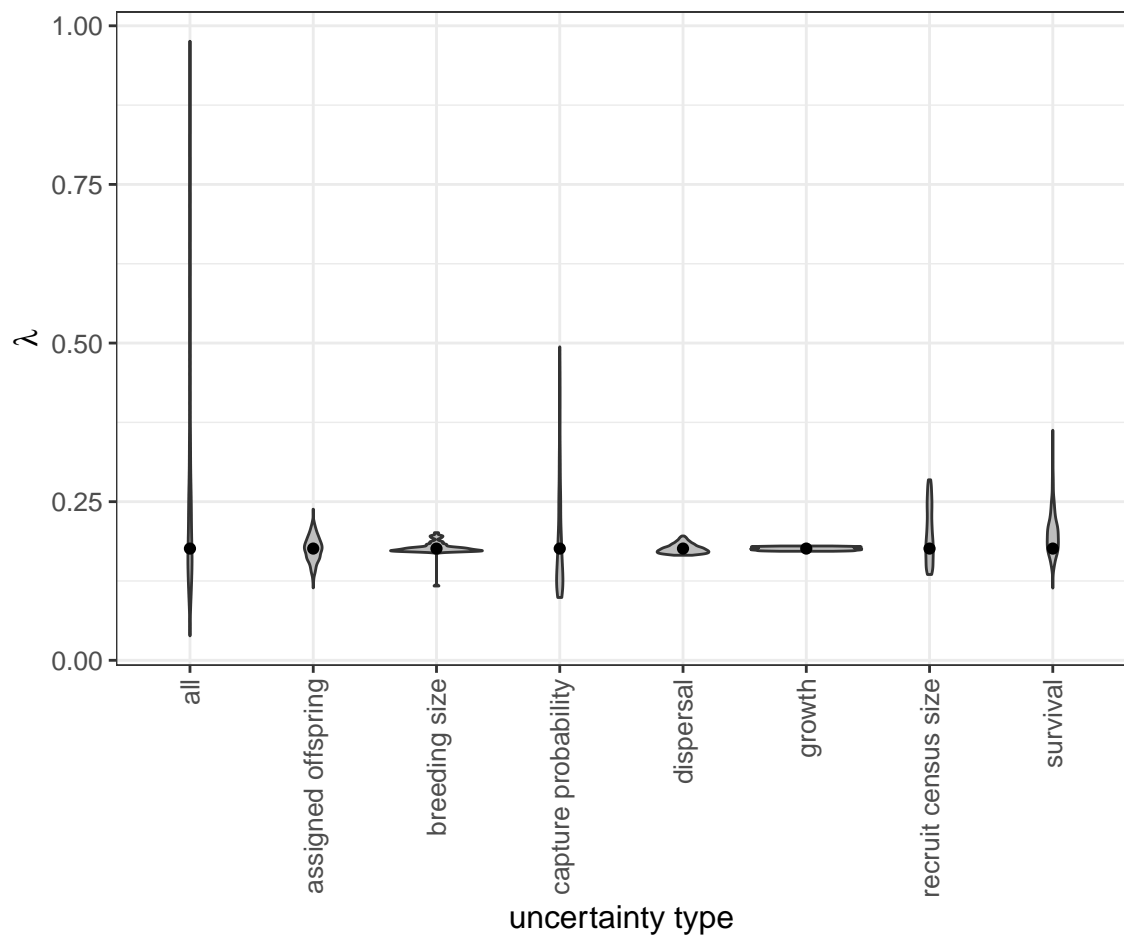


Figure D.14: The contribution of different sources of uncertainty in NP.

References

- Glenn R Almany, Serge Planes, Simon R Thorrold, Michael L Berumen, Michael Bode, Pablo Saenz-Agudelo, Mary C Bonin, Ashley J Frisch, Hugo B Harrison, Vanessa Messmer, et al. Larval fish dispersal in a coral-reef seascape. *Nature Ecology & Evolution*, 1:0148, 2017.
- Michael Arvedlund, Mark I McCormick, Daphne G Fautin, and Mogens Bildsøe. Host recognition and possible imprinting in the anemonefish *amphiprion melanopus* (pisces: Pomacentridae). *Marine Ecology Progress Series*, 188:207–218, 1999.
- Diana S Baetscher, Eric C Anderson, Elizabeth A Gilbert-Horvath, Daniel P Malone, Emily T Saarman, Mark H Carr, and John Carlos Garza. Dispersal of a nearshore marine fish connects marine reserves and adjacent fished areas along an open coast. *Molecular ecology*, 28(7):1611–1623, 2019.
- Douglas Bates, Martin Mächler, Ben Bolker, and Steve Walker. Fitting linear mixed-effects models using lme4. *Journal of Statistical Software*, 67(1):1–48, 2015. doi: 10.18637/jss.v067.i01.
- David R Bellwood and Rebecca Fisher. Relative swimming speeds in reef fish larvae. *Marine Ecology Progress Series*, 211:299–303, 2001.
- Michael Bode, David H Williamson, Hugo B Harrison, Nick Outram, and Geoffrey P Jones. Estimating dispersal kernels using genetic parentage data. *Methods in Ecology and Evolution*, 9(3):490–501, 2018.

Michael Bode, Jeffrey M. Leis, Luciano B. Mason, David H. Williamson, Hugo B. Harrison, Severine Choukroun, and Geoffrey P. Jones. Successful validation of a larval dispersal model using genetic parentage data. *PLOS Biology*, 17(7):1–13, 07 2019. doi: 10.1371/journal.pbio.3000380. URL <https://doi.org/10.1371/journal.pbio.3000380>.

Louis W. Botsford, Alan Hastings, and Steven D. Gaines. Dependence of sustainability on the configuration of marine reserves and larval dispersal distance. *Ecology Letters*, 4:144–150, 2001.

Louis W Botsford, J Wilson White, and Alan Hastings. *Population Dynamics for Conservation*. Oxford University Press, 2019.

Scott C Burgess, Kerry J Nickols, Chris D Griesemer, Lewis AK Barnett, Allison G Dedrick, Erin V Satterthwaite, Lauren Yamane, Steven G Morgan, J Wilson White, and Louis W Botsford. Beyond connectivity: how empirical methods can quantify population persistence to improve marine protected-area design. *Ecological Applications*, 24(2):257–270, 2014.

Peter Buston. Forcible eviction and prevention of recruitment in the clown anemonefish. *Behavioral Ecology*, 14(4):576–582, 2003a.

Peter Buston. Social hierarchies: size and growth modification in clownfish. *Nature*, 424(6945):145–146, 2003b.

Peter M Buston and Cassidy C DAloia. Marine ecology: reaping the benefits of local dispersal. *Current Biology*, 23(9):R351–R353, 2013.

Peter M Buston and Jane Elith. Determinants of reproductive success in dominant pairs of clownfish: a boosted regression tree analysis. *Journal of Animal Ecology*, 80(3):528–538, 2011.

Peter M Buston, Geoffrey P Jones, Serge Planes, and Simon R Thorrold. Probability of successful larval dispersal declines fivefold over 1 km in a coral reef fish. *Proceedings of the Royal Society of London B: Biological Sciences*, page rspb20112041, 2011.

Henry S Carson, Geoffrey S Cook, Paola C López-Duarte, and Lisa A Levin. Evaluating the importance of demographic connectivity in a marine metapopulation. *Ecology*, 92(10):1972–1984, 2011.

Max C. N. Castorani, Daniel C. Reed, Filipe Alberto, Tom W. Bell, Rachel D. Simons, Kyle C. Cavanaugh, David A. Siegel, and Peter T. Raimondi. Connectivity structures local population dynamics: a long-term empirical test in a large metapopulation system. *Ecology*, 96(12):3141–3152, December 2015. ISSN 0012-9658. doi: 10.1890/15-0283.1. URL <http://www.esajournals.org/doi/10.1890/15-0283.1>.

Katrina A Catalano, Allison G Dedrick, Michelle Stuart, Jonathan Purtiz, Humberto Montes, Jr., and Malin Pinsky. Interannual variability of genetic connectivity in a coral reef fish *Amphiprion clarkii*. in prep.

Joshua E Cinner, Cindy Huchery, M Aaron MacNeil, Nicholas AJ Graham, Tim R McClanahan, Joseph Maina, Eva Maire, John N Kittinger, Christina C Hicks,

Camilo Mora, et al. Bright spots among the worlds coral reefs. *Nature*, 535(7612): 416–419, 2016.

MA Coleman, P Cetina-Heredia, M Roughan, M Feng, E van Sebille, and BP Kealaher. Anticipating changes to future connectivity within a network of marine protected areas. *Global Change Biology*, 2017.

C. C. D'Aloia, S. M. Bogdanowicz, J. E. Majoris, R. G. Harrison, and P. M. Buston. Self-recruitment in a Caribbean reef fish: a method for approximating dispersal kernels accounting for seascape. *Molecular Ecology*, 22(9):2563–2572, May 2013. ISSN 09621083. doi: 10.1111/mec.12274. URL <http://doi.wiley.com/10.1111/mec.12274>.

JK Elliott, JM Elliott, and RN Mariscal. Host selection, location, and association behaviors of anemonefishes in field settlement experiments. *Marine Biology*, 122 (3):377–389, 1995.

Stephen P Ellner, Dylan Z Childs, Mark Rees, et al. Data-driven modelling of structured populations. *A practical guide to the Integral Projection Model*. Cham: Springer, 2016.

Lenore Fahrig. How much habitat is enough? *Biological conservation*, 100(1):65–74, 2001.

Daphne Gail Fautin, Gerald R Allen, Gerald Robert Allen, Australia Naturalist, Gerald Robert Allen, and Australie Naturaliste. Field guide to anemonefishes and their host sea anemones. 1992.

Will F Figueira. Connectivity or demography: defining sources and sinks in coral reef fish metapopulations. *Ecological Modelling*, 220(8):1126–1137, 2009.

Will F Figueira and Larry B Crowder. Defining patch contribution in source-sink metapopulations: the importance of including dispersal and its relevance to marine systems. *Population Ecology*, 48(3):215–224, 2006.

Rebecca Fisher. Swimming speeds of larval coral reef fishes: impacts on self-recruitment and dispersal. *Marine Ecology Progress Series*, 285:223–232, 2005.

Emma Fuller, Eleanor Brush, and Malin L Pinsky. The persistence of populations facing climate shifts and harvest. *Ecosphere*, 6(9):1–16, 2015.

Lysel Garavelli, J Wilson White, Iliana Chollett, and Laurent Marcel Chérubin. Population models reveal unexpected patterns of local persistence despite widespread larval dispersal in a highly exploited species. *Conservation Letters*, 11(5):e12567, 2018.

Sarah O Hameed, J Wilson White, Seth H Miller, Kerry J Nickols, and Steven G Morgan. Inverse approach to estimating larval dispersal reveals limited population connectivity along 700 km of wave-swept open coast. *Proceedings of the Royal Society B: Biological Sciences*, 283(1833):20160370, 2016.

Ilkka Hanski. Metapopulation dynamics. *Nature*, 396(6706):41–49, 1998.

Kyle E Harms, S Joseph Wright, Osvaldo Calderón, Andres Hernandez, and Ed-

ward Allen Herre. Pervasive density-dependent recruitment enhances seedling diversity in a tropical forest. *Nature*, 404(6777):493–495, 2000.

Deborah R Hart and Antonie S Chute. Estimating von bertalanffy growth parameters from growth increment data using a linear mixed-effects model, with an application to the sea scallop *placopecten magellanicus*. *ICES Journal of Marine Science*, 66(10):2165–2175, 2009.

Alan Hastings and Louis W. Botsford. Persistence of spatial populations depends on returning home. *Proceedings of the National Academy of Sciences*, 103:6067–6072, 2006.

Akihisa Hattori and Yasunobu Yanagisawa. Life-history pathways in relation to gonadal sex differentiation in the anemonefish, *amphiprion clarkii*, in temperate waters of japan. *Environmental Biology of Fishes*, 31(2):139–155, 1991.

Kina Hayashi, Katsunori Tachihara, and James Davis Reimer. Low density populations of anemonefish with low replenishment rates on a reef edge with anthropogenic impacts. *Environmental Biology of Fishes*, 102(1):41–54, 2019.

Robert J. Hijmans. *geosphere: Spherical Trigonometry*, 2017. URL <https://CRAN.R-project.org/package=geosphere>. R package version 1.5-7.

Jordan N. Holtswarth, Shem B. San Jose, Humberto R. Montes Jr., James W. Morley, and Malin. L Pinsky. The reproductive seasonality and fecundity of yellowtail clownfish (*amphiprion clarkii*) off the philippines. *Bulletin of Marine Science*, 93, 2017.

Darren W Johnson, Mark R Christie, Timothy J Pusack, Christopher D Stallings, and Mark A Hixon. Integrating larval connectivity with local demography reveals regional dynamics of a marine metapopulation. *Ecology*, 99(6):1419–1429, 2018.

Mark P Johnson. Metapopulation dynamics of *tigriopus brevicornis* (harpacticoida) in intertidal rock pools. *Marine Ecology Progress Series*, 211:215–224, 2001.

David M. Kaplan, Louis W. Botsford, Michael R. O’Farrell, Steven D. Gaines, and Salvador Jorgensen. Model-based assessment of persistence in proposed marine protected area designs. *Ecological Applications*, 19(2):433–448, March 2009. ISSN 1051-0761. doi: 10.1890/07-1705.1. URL <http://www.esajournals.org/doi/abs/10.1890/07-1705.1>.

Jacob P Kritzer and Peter F Sale. *Marine metapopulations*. Elsevier Academic Press, 2006.

J.L. Laake. RMark: An r interface for analysis of capture-recapture data with MARK. AFSC Processed Rep. 2013-01, Alaska Fish. Sci. Cent., NOAA, Natl. Mar. Fish. Serv., Seattle, WA, 2013. URL <http://www.afsc.noaa.gov/Publications/ProcRpt/PR2013-01.pdf>.

David Lecchini, Serge Planes, and René Galzin. Experimental assessment of sensory modalities of coral-reef fish larvae in the recognition of their settlement habitat. *Behavioral Ecology and Sociobiology*, 58(1):18–26, 2005.

Dale R Lockwood, Alan Hastings, and Louis W Botsford. The effects of dispersal

patterns on marine reserves: does the tail wag the dog? *Theoretical population biology*, 61(3):297–309, 2002.

Atte Moilanen, Andrew T Smith, and Ilkka Hanski. Long-term dynamics in a metapopulation of the american pika. *The American Naturalist*, 152(4):530–542, 1998.

Piotr Nowicki and Vladimir Vrabec. Evidence for positive density-dependent emigration in butterfly metapopulations. *Oecologia*, 167(3):657, 2011.

Piotr Nowicki, Simona Bonelli, Francesca Barbero, and Emilio Balletto. Relative importance of density-dependent regulation and environmental stochasticity for butterfly population dynamics. *Oecologia*, 161(2):227–239, 2009.

Haruki Ochi. Mating behavior and sex change of the anemonefish, *amphiprion clarkii*, in the temperate waters of southern japan. *Environmental Biology of Fishes*, 26(4):257–275, 1989.

Malin L Pinsky, Humberto R Montes Jr, and Stephen R Palumbi. Using isolation by distance and effective density to estimate dispersal scales in anemonefish. *Evolution*, 64(9):2688–2700, 2010.

BJ Puckett and DB Eggleston. Metapopulation dynamics guide marine reserve design: importance of connectivity, demographics, and stock enhancement. *Ecosphere*, 7(6), 2016.

H Ronald Pulliam. Sources, sinks, and population regulation. *The American Naturalist*, 132(5):652–661, 1988.

Nicholas L Rodenhouse, T Scott Sillett, Patrick J Doran, and Richard T Holmes. Multiple density-dependence mechanisms regulate a migratory bird population during the breeding season. *Proceedings of the Royal Society of London. Series B: Biological Sciences*, 270(1529):2105–2110, 2003.

Pablo Saenz-Agudelo, Geoffrey P Jones, Simon R Thorrold, and Serge Planes. Connectivity dominates larval replenishment in a coastal reef fish metapopulation. *Proceedings of the Royal Society of London B: Biological Sciences*, 278(1720):2954–2961, 2011.

Océane C Salles, Glenn R Almany, Michael L Berumen, Geoffrey P Jones, Pablo Saenz-Agudelo, Maya Srinivasan, Simon R Thorrold, Benoit Pujol, and Serge Planes. Strong habitat and weak genetic effects shape the lifetime reproductive success in a wild clownfish population. *Ecology letters*, 23(2):265–273, 2020.

Océane C. Salles, Jeffrey A. Maynard, Marc Joannides, Corentin M. Barbu, Pablo Saenz-Agudelo, Glenn R. Almany, Michael L. Berumen, Simon R. Thorrold, Geoffrey P. Jones, and Serge Planes. Coral reef fish populations can persist without immigration. *Proceedings of the Royal Society B: Biological Sciences*, 282(1819):20151311, November 2015. ISSN 0962-8452, 1471-2954. doi: 10.1098/rspb.2015.1311. URL <http://rspb.royalsocietypublishing.org/lookup/doi/10.1098/rspb.2015.1311>.

R Kent Smedbol, Arran McPherson, Michael M Hansen, and Ellen Kenchington. Myths and moderation in marine metapopulations? *Fish and Fisheries*, 3(1):20–35, 2002.

James NM Smith and Jessica J Hellmann. Population persistence in fragmented landscapes. *Trends in Ecology & Evolution*, 17(9):397–399, 2002.

Diane M Thompson, J Kleypas, F Castruccio, Enrique N Curchitser, Malin L Pinsky, B Jönsson, and James R Watson. Variability in oceanographic barriers to coral larval dispersal: Do currents shape biodiversity? *Progress in oceanography*, 165: 110–122, 2018.

Nick Tolimieri and Phillip S Levin. The roles of fishing and climate in the population dynamics of bocaccio rockfish. *Ecological Applications*, 15(2):458–468, 2005.

Mark JA Vermeij and Stuart A Sandin. Density-dependent settlement and mortality structure the earliest life phases of a coral population. *Ecology*, 89(7):1994–2004, 2008.

Robert R Warner and Peter L Chesson. Coexistence mediated by recruitment fluctuations: a field guide to the storage effect. *The American Naturalist*, 125(6): 769–787, 1985.

J Wilson White and Jameal F Samhouri. Oceanographic coupling across three trophic levels shapes source–sink dynamics in marine metacommunities. *Oikos*, 120(8): 1151–1164, 2011.

J. Wilson White, Mark H Carr, Jennifer E Caselle, Libe Washburn, C. Brock Woodson, Stephen R Palumbi, Peter M Carlson, Robert R Warner, Bruce A Menge, John A Barth, Carol A Blanchette, Peter T Raimondi, and Kristen Milligan. Connectivity, dispersal, and recruitment: Connecting benthic communities and the coastal ocean. *Oceanography*, 32(3):50–59, 2019.

Jw White, Lw Botsford, A Hastings, and Jl Largier. Population persistence in marine reserve networks: incorporating spatial heterogeneities in larval dispersal. *Marine Ecology Progress Series*, 398:49–67, January 2010. ISSN 0171-8630, 1616-1599. doi: 10.3354/meps08327. URL <http://www.int-res.com/abstracts/meps/v398/p49-67/>.

Adam Yawdoszyn. Fecundity in clownfish. in prep.